Bone marrow macrophages contribute to diabetic stem cell mobilopathy by producing Oncostatin M

Running title

"Macrophages prevent stem cell mobilization"

Authors

Mattia Albiero[1,2], Nicol Poncina[1,2], Stefano Ciciliot[1,2], Roberta Cappellari[1], Lisa Menegazzo[1,2], Francesca Ferraro[3,4], Chiara Bolego[5], Andrea Cignarella[1], Angelo Avogaro[1,2], Gian Paolo Fadini[1,2]

Affiliations

[1]Department of Medicine, University of Padova

[2]Venetian Institute of Molecular Medicine, Padova

[3]Pennsylvania Hospital, University of Pennsylvania Health System

[4]Fox Chase Cancer Center, Philadelphia, USA

[5]Department of Pharmaceutical Sciences, University of Padova

Corresponding author

Gian Paolo Fadini, MD PhD

Assistant Professor of Endocrinology and Metabolism

Department of Medicine, Division of Metabolic Diseases

University Hospital of Padova (Italy)

Phone: +39-049-8214318; Fax: +39-049-8212184

gianpaolofadini@hotmail.com

gianpaolo.fadini@unipd.it

Word count: 3,936

1 Table, 6 Figures

The manuscript has an online data supplement

ABSTRACT

Diabetes affects bone marrow (BM) structure and impairs mobilization of stem cells (SC) into peripheral blood (PB). This amplifies multiorgan complications because BMSC promote vascular repair. As diabetes skews macrophage phenotypes and BM macrophages (BMMΦ) prevent SC mobilization, we hypothesized that excess BMMΦ contribute to diabetic SC mobilopathy. We show that diabetic patients have increased M1 macrophages, while diabetic mice have increased $CD169^+$ BMMΦ with SC retaining activity. Depletion of BMMΦ restored SC mobilization in diabetic mice. We found that CD169 labels M1 macrophages and that conditioned medium (CM) from M1, but not from M0 and M2, macrophages induced CXCL12 expression by MSCs. In silico data mining and in vitro validation identified Oncostatin M (OSM) as the soluble mediator contained in M1 CM that induces CXCL12 expression, via a MEK-p38-STAT3 dependent pathway. In diabetic mice, OSM neutralization prevented CXCL12 induction, improved G-CSF and ischemia-induced mobilization, SC homing to ischemic muscles, and vascular recovery. In diabetic patients, BM plasma OSM levels were higher and correlated with the BM-to-PB SC ratio. In conclusion, BMMΦ prevent SC mobilization by OSM secretion, and OSM antagonism is a target to restore BM function in diabetes, which can translate into vascular protection mediated by BMSC.

INTRODUCTION

Diabetes leads to multiorgan pathology which ultimate reduces life expectancy (1). A series of consistent studies carried out in animals and humans indicate that diabetes affects structure and function of the bone marrow (BM) (2). Extensive remodeling of the BM microvasculature has been demonstrated in mice (3) and patients (4) with diabetes. Along with autonomic neuropathy (5), such profound alterations in the stem cell (SC) niche cause BM dysfunction, evidenced by an impaired SC mobilization in response to ischemia (6; 7) and granulocyte-colony stimulation factor (G-CSF) (8; 9). This novel type of chronic diabetic complication, deemed "stem cell mobilopathy" (10), has implications for the care of diabetic patients with hematological disorders. In addition, as the BM is a reservoir of vascular regenerative cells, BM alterations may pave the way to multiorgan damage (2).

On a molecular level, diabetes prevents the CXCL12 switch (11; 12), i.e. the suppression of intramarrow levels of the chemokine CXCL12 that normally allows stem cell mobilization (13). Although a maladaptive response of the CXCL12-cleaving enzyme DPP-4 has been hypothesized (14), the exact mechanism perturbing a coordinated CXCL12 regulation in diabetes is unclear. We have previously shown that by-passing BM neuronal control, through sympathetic nervous system (SNS)-independent stimuli, restores SC mobilization in diabetes (5). Indeed, diabetic mice can be effectively mobilized by the clinical-grade CXCR4 antagonist AMD3100/Plerixafor, which desensitizes SC to CXCL12, thereby letting them leave the BM and reach the systemic circulation (15). Although the mobilizing activity of G-CSF is partly mediated by the SNS (16), G-CSF signals primarily via a receptor expressed on $CD68^+$ macrophages (17), and macrophage suppression is essential to induce SC mobilization (18). Intramarrow macrophages expressing CD169 (Siglec-1) have been shown to secrete a hitherto unknown soluble protein that increases the expression and release of CXCL12 by mesenchymal stem/stromal cells (MSC), providing a strong retention signal for SC in the marrow (19). Identification of such macrophage-derived factor is a primary challenge

in this field, as it will eventually turn into a therapeutic target in "poor mobilizer" conditions, such as diabetes. Based on the observations that hyperglycemia promotes myelopoiesis (20), diabetes alters macrophage populations (21), and is associated with a defective CXCL12 switch (11; 12), we herein examined the role of BM macrophages in the diabetic SC mobilopathy. We found an excess of pro-inflammatory macrophages in the diabetic BM, and that macrophage depletion restores mobilization. We also describe the discovery that Oncostatin M (OSM) is the long sought soluble factor released by macrophages that sustains CXCL12 expression by MSCs. Neutralization of OSM is therefore a candidate therapy to restore SC mobilization and vascular repair in diabetes.

MATERIAL AND METHODS

Patients. All protocols involving patients were approved by the local ethical committee and carried out in accordance with the principles of the Declaration of Helsinki as revised in 2008. All subjects provided written informed consent. Type 1 diabetic (T1D) patients were recruited from the outpatient diabetes clinic of the University Hospital of Padova, whereas non diabetic subjects were selected among individuals presenting for a cardiometabolic screening. Details on inclusion / exclusion criteria and clinical characterization of patients are provided in the online data supplement. Enrolment in the BM stimulation protocol and treatment with G-CSF in the trial NCT01102699 are described elsewhere (9). Coupled peripheral blood and BM samples were collected from patients undergoing hip replacement surgery.

Animals. All procedures were approved by the local ethic committee and from the Italian Ministry of Health. Experiments were conducted according to the "Principles of laboratory animal care" (NIH publication no. 85–23,4 revised 1985). All animals were on a C57BL/6 background. Diabetes was induced with a single injection of streptozotocin. Additional details are provided in the online data supplement.

Mobilization assays. The following mobilization assays were used: i) 4 day s.c. G-CSF course; ii) clodronate liposome injection eventually followed by a G-CSF course; iii) Antibody-mediated Oncostatin M neutralization, followed by a G-CSF course. Details are provided in the online data supplement.

FACS analysis. Human circulating monocyte-macrophages were identified and quantified as previously described (21). M1 were defined as $CD68^+CCR2^+$ cells and M2 were defined as $CX3CR1^+CD163^+/CD206^+$. Baseline and post-G-CSF levels of circulating $CD34^+$ stem cells were

quantified as previously described (9). For identification of murine BM macrophage phenotypes we used the protocol described by Chow et al. (19). Macrophages were identified in the Gr-1^{neg}/$CD115^{neg}$ gate as cells expressing the macrophage marker F4/80 with low side scatter, In parallel experiments, macrophages were also identified as cells that co-expressed F4/80 and MHC-II in the $CD45^{+}Gr\text{-}1^{-}$ gate. Mouse progenitor cell levels were quantified in peripheral blood before and after mobilization: cells were stained with APC-lineage cocktail, PE anti Sca-1 and FITC anti cKit to quantify LKS cells or with Alexa647 anti-CD34 and Alexa488 anti Flk-1 to quantify endothelial progenitor cells. Additional details are provided in the online data supplement.

Cell cultures. Human monocyte-derived macrophages were obtained as previously described (21): resting M0 cells were polarized into M1 or M2 macrophages by 48h incubation with LPS and IFN-γ or IL-4 and IL-13, respectively. After 48h, the medium was removed, macrophages kept in serum-free RPMI for further 72h, then conditioned media (CM) were harvested. Human bone marrow MSCs were obtain from the BM of patients undergoing orthopedic surgery at the University Hospital of Padova. BM aspirate pellets were plated on TC Petri dishes with mesenchymal medium. Murine MSCs were obtained by from C56Bl6/J mice: femurs and tibia were flushed with ice cold PBS, and cells cultured in MEM-alpha. Murine macrophages were obtained from BM cells cultured in RPMI-1640 supplemented with M-CSF for 7 days and then polarized for 48h with LPS and IFN-γ (M1) or IL-4 and IL-13 (M2).

Gene expression analyses. Total RNA was extracted using Trizol® reagent following the manufacturer's protocol. RNA was reverse transcribed using the First-Strand cDNA Synthesis Kit and duplicates sample cDNA were amplified on the 7900HT Fast Real-Time PCR System. Expression data were normalized to the mean of housekeeping gene ubiquitin C. Additional data can be found in the online data supplement.

In vitro CXCL12 assays. Human and mouse MSCs at 90% confluence were incubated with cytokines or CM. CM were incubated with anti-Oncostatin M antibodies, mouse anti-human and rabbit anti-mouse (MAB295 and AF-495-NA respectively; R&D). All experiments were conducted for 48h and then cells were lysed with Trizol for gene expression analysis. Additional details are provided in the online data supplement.

In silico analyses. In silico analyses were performed retrieving gene expression data of human and mouse macrophages and MSCs from GEO database series. Murine and human expression data were both divided in two different groups: (M(-) or M0 vs M(IFNγ+LPS) or M1 and M(IL4) or M2 vs M(IFNγ+LPS) or M1; and then analyzed using GEO2R tool. We subsequently filtered data according to these stringent criteria: being upregulated in M(IFNγ+LPS) versus M(-) and versus M(IL4) macrophages at least 5 folds (logFC>2.32), and with an adjusted p-value<0.001, in both groups. The two groups where then crossed, to get a list of genes commonly upregulated in M(IFNγ+LPS) macrophages. To select genes encoding for secreted proteins, data were further filtered by comparing the human and murine gene lists obtained as above with a species-specific secreted protein list from the Metazoa Secretome and Subcellular Proteome Knowledgebase. We then manually checked for proteins having a receptor expressed in MSCs according to relevant GEO series. Technical details on this method can be found in the online appendix.

Statistical analysis. Data are expressed as mean±standard error, or as percentage. Normality was checked using the Kolmogorov-Smirnov test and non normal data were log transformed prior to analysis. Comparison between 2 or more groups was performed using the Student's t test and ANOVA for normal variables or using the Mann-Whitney's U test and Kruskall-Wallis test for non normal variables. Linear correlations were checked using the Pearson's r coefficient. Statistical analysis was accepted at $p<0.05$.

RESULTS

Macrophage phenotypes and stem cell mobilization in type 1 diabetic patients.

We have previously shown that pre-diabetes and type 2 diabetes are associated with imbalances in circulating monocyte-macrophage phenotypes, reflecting a disequilibrium in BM populations (21; 22). We herein report that type 1 diabetic (T1D) patients have a significant increase in circulating $CD68^+CCR2^+$ M1-like (pro-inflammatory) macrophages compared to matched controls (clinical characteristics in Table 1). This was attributable to a significant increase in CD68 and, to a lesser extent, CCR2 expression on monocytes of T1D patients (Figure 1A,B). Furthermore, in T1D patients undergoing BM stimulation with G-CSF in the NCT01102699 study (9), there was a strong negative correlation between the degree of $CD34^+$ SC mobilization and the change in $CX3CR1^+CD163^+/CD206^+$ M2-like monocyte-macrophages, which was not observed in non-diabetic controls (Figure 1C). These observations prompted us to explore the role of BM macrophages in the diabetic SC mobilopathy.

BM macrophages in type 1 diabetic mice.

We first examined the percentages of macrophages in the BM of streptozotocin-induced diabetic (T1D) and non-diabetic mice. Both the $Gr1^-CD115^-F4/80^+SSC^{low}$ and $CD45^+Gr1^-MHC\text{-}II^+F4/80^+$ macrophage phenotypes were >2-fold increased by diabetes (Figure 2A,B). Such increase in BM macrophages appears to be independent from sympathetic innervation and from Sirt1 downregulation, which have been previously shown to mediate diabetic BM dysfunction (5): indeed, chemical sympathectomy with 6-OHDA or hematopoietic Sirt1 knockout did not affect the percentages of BM macrophages (Suppl Fig. 1). $Gr1^-CD115^-F4/80^+SSC^{low}$ cells were further characterized by FACS for the expression of classical M1 (CD86) and M2 (scavenger receptors CD301 and CD206) macrophage markers. Although CD301 was slightly more expressed on BM macrophages from diabetic mice, there was no obvious prevalence of M1 vs M2 markers (Figure

2C). Gene expression analysis also did not allow to unequivocally define $Gr1^{-}CD115^{-}F4/80^{+}SSC^{low}$ cells as M1 or M2 (Figure 2D). BM $Gr1^{-}CD115^{-}F4/80^{+}SSC^{low}$ macrophages of diabetic mice showed significantly higher surface and gene expression of CD169 (Figure 2E), which preferentially labels BM macrophages compared to other cell populations (Suppl Fig. 2), and identifies macrophages provided with SC retaining activity in mice and humans (19; 23).

Excess BM macrophage contribute to stem cell mobilopathy in diabetic mice.

In non-diabetic mice, the ability of G-CSF to suppress BM macrophage content is supposed to mediate its mobilizing activity by lifting the inhibitory signal provided by CXCL12 of mesenchymal origin (17; 18). We found that, while G-CSF reduced BM macrophages by about 80% in non-diabetic mice, suppression of BM macrophage content in diabetic mice was <40% and the percentage of post-G-CSF BM macrophages was >5-fold higher in diabetic compared to non-diabetic mice (Figure 3A). Therefore, we hypothesized that SC mobilization failure in response to G-CSF in diabetic mice is attributable, at least in part, to excess BM macrophage content. To clarify this point, we depleted BM macrophages using clodronate liposomes, which kill phagocytic cells by delivering toxic intracellular concentrations of clodronate (24). This approach effectively and equally depleted BM macrophages and abated BM CXCL12 gene expression in both non-diabetic and diabetic mice (Figure 3B,C). Peripheral blood macrophages and $Gr\text{-}1^{high}$ monocytes were also depleted, but neutrophils were unaffected. Among other niche genes, clodronate liposome treatment also reduced Vcam1 expression (Suppl Fig 3A,B), As a result, spontaneous and G-CSF induced mobilization of LKS and $CD34^{+}Flk\text{-}1^{+}$ SC was restored toward normal levels in diabetic mice (Figure 3D,E). These data confirm that excess BM macrophages contribute to SC mobilopathy in diabetes. However, an unrestricted targeting of BM macrophages with clodronate liposomes is unlikely to be a suitable therapeutic approach to restore BM function, as it can have negative off-target effects. We therefore sought to identify the hitherto unknown soluble factor released by macrophages that prevents SC mobilization.

M1 macrophages provide stem cell retention signals.

To better understand the meaning of CD169 overexpression in diabetic macrophages, we performed an in silico analysis of the expression of CD169 probes in the public GEO dataset GDS2429, reporting gene expression profiles during typical M1 (IFNγ+LPS) and M2 (IL-4) macrophage polarization from human monocytes (Figure 4A). CD169 was confirmed as a macrophage marker, as its expression markedly increased during monocytes-macrophage differentiation, and was much more expressed in M1 compared to M0 and M2 macrophages (Figure 4B). To validate this finding, we obtained human M0, M1 and M2 macrophages using the same in vitro polarization protocol. Polarization efficiency was verified by upregulation of M1 genes Il1b, Tnfa and iNos and downregulation of Mrc1/CD206 in cells treated with IFNγ+LPS compared with cells treated with IL-4 (Suppl Fig. 4). CD169 was more expressed in M1 compared to M0 and M2 by both FACS and qPCR (Figure 4C,D). These data indicate that CD169 is a marker of the pro-inflammatory M1 macrophage phenotype.

The macrophage conditioned medium (CM) is known to increase expression and release of the retention chemokine CXCL12 by BM MSCs, thereby preventing SC mobilization (19). We therefore obtained CM from M0, M1 and M2 human macrophages, and cultured human BM-derived MSCs, most of which expressed Nestin (Figure 4E), a niche-supporting cell marker (25). After incubating $Nestin^+$ MSCs with macrophage CM for 48 hours, we found that only CM from M1, but not from M0 and M2 macrophages, induced CXCL12 expression in MSCs (Figure 4E). Among other niche genes, we found that M1 CM increased Angpt1 and Kitl expression (Suppl Fig. 5). This finding, which was consistently reproducible using different batches of CM and different MSC donors, suggests that only pro-inflammatory macrophages (M1) promote retention versus mobilization of BMSC through the secretion of a soluble mediator. In further support, by using mouse BM-derived macrophages polarized into M1 and M2, as well as mouse BM MSCs, we

confirmed that M1 macrophages express higher CD169 levels and M1, but not M0 and M2 CM, induces CXCL12 expression (Suppl Fig. 6A-C).

Macrophage-derived oncostatin M promotes CXCL12 expression.

The effect of M1 CM on CXCL12 expression by MSCs was completely abolished by proteinase K, but not by a protease inhibitor (Figure 4F,G), suggesting that the M1, but not the M0 and M2 CM, contains a protein that signals in MSCs and stimulates CXCL12 expression. In order to discover such soluble factor, we performed an in silico analysis of the public gene expression profiles of human and mouse polarized macrophages and MSCs (Suppl Fig. 7A). Genes that were significantly upregulated in M1 compared to M0 and M2 were screened for those encoding secreted factors having a receptor expressed on BM-derived MSCs. A list of candidate human and mouse genes/proteins was thus retrieved and scored by a literature search, looking at soluble factors produced by inflammatory macrophages that may induce CXCL12 expression by MSCs. Final candidates were validated *in vitro* by a dose-response stimulation of MSCs (Suppl Fig. 7B). After unsuccessful testing of several candidates (CXCL10, CXCL11, TNF-α, PDGF-A, IL-15, and ET-1; Suppl Fig. 8), we found that Oncostatin M (OSM) was able to exponentially increase CXCL12 expression by MSCs (Figure 5A). The other gp130 ligands, namely IL-6 and LIF, did not exert the same CXCL12 inducing effect (Suppl Fig. 9). As measured by ELISA, OSM protein concentrations were markedly higher in the CM of mouse and human M1 compared to M0 and M2 (Figure 5B and Suppl Fig. 6D), and OSM gene expression was several times upregulated in M1 vs M0 and M2 macrophages (Figure 5C). Gene expression levels of OSM in the BM was significantly reduced after treatment with clodronate liposomes in diabetic and non diabetic mice (Figure 5D).

Thus, we focused on OSM as the most likely candidate stem cell retention factor produced by BM macrophages. Incubation of human MSCs with CM from human M1 in the presence of a neutralizing anti-human OSM monoclonal antibody completely abolished the effect on CXCL12 expression (Figure 5E). This confirmed that OSM is the soluble factor contained in M1 CM that

stimulates CXCL12 expression by MSCs. CXCL12 induction by OSM was confirmed in other cell types, such as endothelial cells (HUVECs and HAECs) and fibroblasts (Suppl Fig 10A). Though microvascular permeability impacts SC mobilization (26), we did not find any effect of OSM on permeability of a HUVEC monolayer (Suppl Fig 10B), suggesting that CXCL12 regulation is the most likely candidate mechanism whereby OSM regulates mobilization. To explore the molecular mechanisms, we analyzed classical pathways activated by OSM receptor. Induction of CXCL12 expression by OSM was abolished when MSCs were co-treated with inhibitors of MEK (U0126), p38 (SB202190), and STAT3 (Stattic) (Suppl Fig 11A). As shown by FACS, STAT3 phosphorylation by OSM was reduced by co-treatment with the p38 inhibitor (Suppl Fig 11B), suggesting a MEK-p38-STAT3 pathway. However, simple p38 or STAT3 activation was insufficient to induce CXCL12 in MSCs (Suppl Fig 11C), suggesting that recruitment of other co-factors by OSM signaling is required.

Oncostatin M neutralization restores SC mobilization, homing, and vascular recovery in diabetes.

For an in vivo validation of the role of OSM as a retention factor, we treated T1D and non-diabetic mice with a neutralizing anti-mouse OSM antibody the day before starting G-CSF stimulation. This protocol abated circulating OSM concentrations and restored a significant CXCL12 gradient switch by G-CSF in diabetic mice, by rising its PB/BM concentration ratio (Suppl Fig 12). While diabetic mice failed to mobilize LKS and $CD34^{+}Flk\text{-}1^{+}$ cells in response to G-CSF alone, OSM neutralization was able to restore G-CSF-induced LKS and $CD34^{+}Flk\text{-}1^{+}$ cell mobilization in diabetic mice to the level seen in non-diabetic mice and beyond (Figure 5F-K). In view of clinical translation, we examined OSM concentrations in relation to peripheral blood (PB) and BM $CD34^{+}$ cell distribution in 6 diabetic and 6 matched non-diabetic individuals (clinical characteristics in Supplemental Table S2). BM plasma OSM concentration and BM/PB $CD34^{+}$ cell ratio were higher

in diabetic patients, and a close direct correlation between these parameters was found, supporting the notion that OSM regulates BM-to-PB stem cell mobilization (Figure 5J-M).

In diabetes, not only G-CSF, but also ischemia-induced mobilization is defective. We therefore sought to verify whether OSM inhibition affects response to ischemia in diabetic mice undergoing hind limb ischemia with or without treatment with the neutralizing anti-OSM antibody. By FACS analysis, we found that OSM neutralization increased the amount of circulating LKS cells after ischemia and restored the amount of LKS homed to the ischemic muscles toward levels seen in non-diabetic mice (Figure 6A,B). In addition, OSM neutralization restored hind limb perfusion 14 days after ischemia, as shown by laser Doppler imaging (Figure 6C).

DISCUSSION

We herein show that excess pro-inflammatory macrophages in the diabetic BM provide a retention signal for SC by secreting OSM and inducing CXCL12 in MSCs. Macrophage depletion and OSM neutralization were indeed able to restore SC mobilization toward normal levels in diabetic mice, which translated into improved vascular recovery after ischemia.

Diabetes induces a profound remodeling in the BMSC niche in mice and humans (3-5; 27), which impairs SC mobilization in response to ischemia and growth factors (6-9). Multiple molecular pathways may mediate this dysfunction, but the exact mechanisms are unknown, thus limiting the possibility to pursue targeted therapies. Based on the notion that diabetes affects the monocyte-macrophage compartment (21; 22; 28), and that macrophages prevent SC mobilization (19), we herein assessed whether BM macrophages contribute to the diabetic SC mobilopathy. Using standardized FACS protocols (19), we found 2-3 fold increased levels of macrophages in the diabetic BM, that were not adequately suppressed by G-CSF. This is in line with the previous finding that hyperglycemia skews SC differentiation to myeloid phenotypes through AGE/RAGE interactions (20). Chow et al. clearly demonstrated that macrophages equipped with SC retention activity are labeled by the adhesion molecule CD169, because selective depletion of $CD169^+$ cells allows SC mobilization. Macrophage in the diabetic BM displayed increased expression of CD169 and we therefore hypothesized that such an excess in BM macrophages blocks SC mobilization in diabetes. To test this hypothesis, we performed macrophage depletion using clodronate liposomes, which selectively kill specialized phagocytic cells in the reticulo-endothelial system, including the BM. Effective suppression of intramarrow macrophages was followed by the release of SC in diabetic mice and restoration of response to G-CSF toward normal levels.

These data suggest that macrophage targeting can therapeutically restore BM function in diabetes. We therefore focused on the hitherto unrecognized signal(s) whereby BM macrophages affect function of the SC niche (29). By an in silico approach, we discovered that OSM is the long sought

soluble factor released by macrophages that induce the retention signal CXCL12 in MSCs, thereby preventing SC mobilization. The process that led us to this discovery was primed by the finding that the adhesion molecule CD169, which labels macrophages provided with retention activity, is markedly upregulated in pro-inflammatory, so-called classically activated M1 or M(LPS+INFγ), compared to resting M0 and M2 or M(IL-4) macrophages. The segregation of CD169 expression and CM activity enabled us to mine the widely available gene expression profiles of human and mouse M0, M1 and M2 cells, in search of candidate secreted factors that signal through receptors expressed on MSCs. Potential candidates, scored by literature searches, were validated by a simple and rapid in vitro assay of CXCL12 induction. Only OSM, but not the other gp130 ligands LIF and IL-6, fulfilled all such requisites, and OSM blockade completely abolished the effects of M1 CM on CXCL12 expression in MSCs. A preliminary study of signaling pathways identified the MEK-p38-STAT3 axis as likely mediating the effect of OSM on CXCL12 expression. Upon an accurate literature review, it appeared that OSM was already known to be induced in classically activated M1 macrophages (30), able to stimulate CXCL12 production by MSCs (31), and possibly involved in SC retention within the BM (32). In addition, gp130 ligands have been shown to be upregulated in the BM of long-standing murine diabetes, whereas genetic deletion of gp130 reverses some pathologic hematopoietic features associated with diabetes (33). Similarly to what we show in the BM, macrophage-derived OSM seems to play a role also in adipose tissue inflammation (34; 35), where SC, the microvasculature, macrophages and adipocytes form a structure resembling the BM niche.

In further support of the role of OSM in macrophage-mediated regulation of SC trafficking, we found that BM OSM expression was significantly suppressed after macrophage depletion. In view of clinical translation, we also found that OSM concentrations were higher in the BM plasma of diabetic compared to non-diabetic patients and was correlated to a surrogate index of steady state mobilization, such as the ratio of $CD34^+$ SC between the BM and PB. As a final proof-of-concept, we show that in vivo OSM neutralization restored the stem cell mobilization response to G-CSF in

diabetic mice. Ischemia-induced mobilization and homing of LKS cells was also improved after treating diabetic mice with the OSM neutralizing antibody, which was associated with restoration of perfusion. This indicates that any eventual peripheral effect of OSM blocking did not prevent SC from homing to ischemic tissues.

These findings have relevant implications for our knowledge of how macrophages regulate the niche and add an important plug to the complicated puzzle of the diabetic BM pathology. The pathological pathway generated by excess BM macrophages seems independent from other typical features of the diabetic BM, such as neuropathy, oxidative stress, and Sirt1 downregulation (5). However, in view of the severe BM remodeling taking place in diabetes, it is not surprising that both macrophage depletion and OSM neutralization, although effective in restoring response to G-CSF, often elicited a blunted mobilization in diabetic compared with non diabetic mice.

On the background of the well known hyperglycemia-driven myelopoiesis (20), our data indicate that generation of pro-inflammatory macrophages represents a key event in BM dysfunction. Identification of OSM as the mediator of macrophage retaining activity has therapeutic implications to revert the diabetic stem cell mobilopathy and, potentially, in other “poor mobilizer” conditions. As BM-derived cells play a major role in diabetic complications (36), restoration of BMSC mobilization with a targeted molecular approach may restore endogenous vascular regenerative capacity and improve the outcome of diabetic patients.

ACKNOWLEDGEMENTS

Author Contributions: MA, SC, NP, LM, FF, researched data. CB, AC researched data and contributed to discussion. AA contributed to discussion and reviewed/edited manuscript. GPF researched data and wrote the manuscript.

GPF is the guarantor of the study and takes responsibility for the contents of the article.

Sources of support. The study was supported by the GR-2010-2301676 grant of the Italian Ministry of Health to GPF and by a European Foundation for the Study of Diabetes (EFSD) / Novartis programme grant to GPF. MA is supported by the Italian Society of Diabetology (SID).

Conflict of interest. GPF, MA and SC are the inventor of a patent pending, hold by the University of Padova, on the use of Oncostatin M inhibition for the induction of stem cell mobilization in diabetes. NP, LM, RC, FF, CB, AC and AA report no conflict of interest.

REFERENCES

1. Seshasai SR, Kaptoge S, Thompson A, Di Angelantonio E, Gao P, Sarwar N, Whincup PH, Mukamal KJ, Gillum RF, Holme I, Njolstad I, Fletcher A, Nilsson P, Lewington S, Collins R, Gudnason V, Thompson SG, Sattar N, Selvin E, Hu FB, Danesh J: Diabetes mellitus, fasting glucose, and risk of cause-specific death. *N Engl J Med* 364:829-841, 2011
2. Fadini GP, Ferraro F, Quaini F, Asahara T, Madeddu P: Concise Review: Diabetes, the Bone Marrow Niche, and Impaired Vascular Regeneration. *Stem Cells Transl Med*, 2014
3. Oikawa A, Siragusa M, Quaini F, Mangialardi G, Katare RG, Caporali A, van Buul JD, van Alphen FP, Graiani G, Spinetti G, Kraenkel N, Prezioso L, Emanueli C, Madeddu P: Diabetes mellitus induces bone marrow microangiopathy. *Arterioscler Thromb Vasc Biol* 30:498-508, 2010
4. Spinetti G, Cordella D, Fortunato O, Sangalli E, Losa S, Gotti A, Carnelli F, Rosa F, Riboldi S, Sessa F, Avolio E, Beltrami AP, Emanueli C, Madeddu P: Global remodeling of the vascular stem cell niche in bone marrow of diabetic patients: implication of the microRNA-155/FOXO3a signaling pathway. *Circ Res* 112:510-522, 2013
5. Albiero M, Poncina N, Tjwa M, Ciciliot S, Menegazzo L, Ceolotto G, Vigili de Kreutzenberg S, Moura R, Giorgio M, Pelicci P, Avogaro A, Fadini GP: Diabetes causes bone marrow autonomic neuropathy and impairs stem cell mobilization via dysregulated p66Shc and Sirt1. *Diabetes* 63:1353-1365, 2014
6. Fadini GP, Sartore S, Schiavon M, Albiero M, Baesso I, Cabrelle A, Agostini C, Avogaro A: Diabetes impairs progenitor cell mobilisation after hindlimb ischaemia-reperfusion injury in rats. *Diabetologia* 49:3075-3084, 2006
7. Ling L, Shen Y, Wang K, Jiang C, Fang C, Ferro A, Kang L, Xu B: Worse clinical outcomes in acute myocardial infarction patients with type 2 diabetes mellitus: relevance to impaired endothelial progenitor cells mobilization. *PLoS One* 7:e50739, 2012
8. Fadini GP, Avogaro A: Diabetes impairs mobilization of stem cells for the treatment of cardiovascular disease: a meta-regression analysis. *Int J Cardiol* 168:892-897, 2013
9. Fadini GP, Albiero M, Vigili de Kreutzenberg S, Boscaro E, Cappellari R, Marescotti M, Poncina N, Agostini C, Avogaro A: Diabetes impairs stem cell and proangiogenic cell mobilization in humans. *Diabetes Care* 36:943-949, 2013
10. DiPersio JF: Diabetic stem-cell "mobilopathy". *N Engl J Med* 365:2536-2538, 2011
11. Tepper OM, Carr J, Allen RJ, Jr., Chang CC, Lin CD, Tanaka R, Gupta SM, Levine JP, Saadeh PB, Warren SM: Decreased circulating progenitor cell number and failed mechanisms of stromal cell-derived factor-1alpha mediated bone marrow mobilization impair diabetic tissue repair. *Diabetes* 59:1974-1983, 2010
12. Ferraro F, Lymperi S, Mendez-Ferrer S, Saez B, Spencer JA, Yeap BY, Masselli E, Graiani G, Prezioso L, Rizzini EL, Mangoni M, Rizzoli V, Sykes SM, Lin CP, Frenette PS, Quaini F, Scadden DT: Diabetes impairs hematopoietic stem cell mobilization by altering niche function. *Sci Transl Med* 3:104ra101, 2011
13. Petit I, Szyper-Kravitz M, Nagler A, Lahav M, Peled A, Habler L, Ponomaryov T, Taichman RS, Arenzana-Seisdedos F, Fujii N, Sandbank J, Zipori D, Lapidot T: G-CSF induces stem cell mobilization by decreasing bone marrow SDF-1 and up-regulating CXCR4. *Nat Immunol* 3:687-694, 2002
14. Fadini GP, Albiero M, Seeger F, Poncina N, Menegazzo L, Angelini A, Castellani C, Thiene G, Agostini C, Cappellari R, Boscaro E, Zeiher A, Dimmeler S, Avogaro A: Stem cell compartmentalization in diabetes and high cardiovascular risk reveals the role of DPP-4 in diabetic stem cell mobilopathy. *Basic Res Cardiol* 108:313, 2013
15. Broxmeyer HE, Orschell CM, Clapp DW, Hangoc G, Cooper S, Plett PA, Liles WC, Li X, Graham-Evans B, Campbell TB, Calandra G, Bridger G, Dale DC, Srour EF: Rapid mobilization of

murine and human hematopoietic stem and progenitor cells with AMD3100, a CXCR4 antagonist. *J Exp Med* 201:1307-1318, 2005
16. Katayama Y, Battista M, Kao WM, Hidalgo A, Peired AJ, Thomas SA, Frenette PS: Signals from the sympathetic nervous system regulate hematopoietic stem cell egress from bone marrow. *Cell* 124:407-421, 2006
17. Christopher MJ, Rao M, Liu F, Woloszynek JR, Link DC: Expression of the G-CSF receptor in monocytic cells is sufficient to mediate hematopoietic progenitor mobilization by G-CSF in mice. *J Exp Med* 208:251-260, 2011
18. Winkler IG, Sims NA, Pettit AR, Barbier V, Nowlan B, Helwani F, Poulton IJ, van Rooijen N, Alexander KA, Raggatt LJ, Levesque JP: Bone marrow macrophages maintain hematopoietic stem cell (HSC) niches and their depletion mobilizes HSCs. *Blood* 116:4815-4828, 2010
19. Chow A, Lucas D, Hidalgo A, Mendez-Ferrer S, Hashimoto D, Scheiermann C, Battista M, Leboeuf M, Prophete C, van Rooijen N, Tanaka M, Merad M, Frenette PS: Bone marrow CD169+ macrophages promote the retention of hematopoietic stem and progenitor cells in the mesenchymal stem cell niche. *J Exp Med* 208:261-271, 2011
20. Nagareddy PR, Murphy AJ, Stirzaker RA, Hu Y, Yu S, Miller RG, Ramkhelawon B, Distel E, Westerterp M, Huang LS, Schmidt AM, Orchard TJ, Fisher EA, Tall AR, Goldberg IJ: Hyperglycemia promotes myelopoiesis and impairs the resolution of atherosclerosis. *Cell Metab* 17:695-708, 2013
21. Fadini GP, de Kreutzenberg SV, Boscaro E, Albiero M, Cappellari R, Krankel N, Landmesser U, Toniolo A, Bolego C, Cignarella A, Seeger F, Dimmeler S, Zeiher A, Agostini C, Avogaro A: An unbalanced monocyte polarisation in peripheral blood and bone marrow of patients with type 2 diabetes has an impact on microangiopathy. *Diabetologia* 56:1856-1866, 2013
22. Fadini GP, Cappellari R, Mazzucato M, Agostini C, Vigili de Kreutzenberg S, Avogaro A: Monocyte-macrophage polarization balance in pre-diabetic individuals. *Acta Diabetol* 50:977-982, 2013
23. Chow A, Huggins M, Ahmed J, Hashimoto D, Lucas D, Kunisaki Y, Pinho S, Leboeuf M, Noizat C, van Rooijen N, Tanaka M, Zhao ZJ, Bergman A, Merad M, Frenette PS: CD169(+) macrophages provide a niche promoting erythropoiesis under homeostasis and stress. *Nat Med* 19:429-436, 2013
24. Van Rooijen N, Sanders A: Liposome mediated depletion of macrophages: mechanism of action, preparation of liposomes and applications. *J Immunol Methods* 174:83-93, 1994
25. Mendez-Ferrer S, Michurina TV, Ferraro F, Mazloom AR, Macarthur BD, Lira SA, Scadden DT, Ma'ayan A, Enikolopov GN, Frenette PS: Mesenchymal and haematopoietic stem cells form a unique bone marrow niche. *Nature* 466:829-834, 2010
26. Mangialardi G, Katare R, Oikawa A, Meloni M, Reni C, Emanueli C, Madeddu P: Diabetes causes bone marrow endothelial barrier dysfunction by activation of the RhoA-Rho-associated kinase signaling pathway. *Arterioscler Thromb Vasc Biol* 33:555-564, 2013
27. Teraa M, Fledderus JO, Rozbeh RI, Leguit RJ, Verhaar MC: Bone marrow microvascular and neuropathic alterations in patients with critical limb ischemia. *Circ Res* 114:311-314, 2014
28. Olefsky JM, Glass CK: Macrophages, inflammation, and insulin resistance. *Annu Rev Physiol* 72:219-246, 2010
29. Bordon Y: Macrophages: bloody regulators. *Nat Rev Immunol* 13:307, 2013
30. Guihard P, Danger Y, Brounais B, David E, Brion R, Delecrin J, Richards CD, Chevalier S, Redini F, Heymann D, Gascan H, Blanchard F: Induction of osteogenesis in mesenchymal stem cells by activated monocytes/macrophages depends on oncostatin M signaling. *Stem Cells* 30:762-772, 2012
31. Lee MJ, Song HY, Kim MR, Sung SM, Jung JS, Kim JH: Oncostatin M stimulates expression of stromal-derived factor-1 in human mesenchymal stem cells. *Int J Biochem Cell Biol* 39:650-659, 2007

32. Minehata K, Takeuchi M, Hirabayashi Y, Inoue T, Donovan PJ, Tanaka M, Miyajima A: Oncostatin m maintains the hematopoietic microenvironment and retains hematopoietic progenitors in the bone marrow. *Int J Hematol* 84:319-327, 2006
33. Hazra S, Jarajapu YP, Stepps V, Caballero S, Thinschmidt JS, Sautina L, Bengtsson N, Licalzi S, Dominguez J, Kern TS, Segal MS, Ash JD, Saban DR, Bartelmez SH, Grant MB: Long-term type 1 diabetes influences haematopoietic stem cells by reducing vascular repair potential and increasing inflammatory monocyte generation in a murine model. *Diabetologia* 56:644-653, 2013
34. Sanchez-Infantes D, White UA, Elks CM, Morrison RF, Gimble JM, Considine RV, Ferrante AW, Ravussin E, Stephens JM: Oncostatin m is produced in adipose tissue and is regulated in conditions of obesity and type 2 diabetes. *J Clin Endocrinol Metab* 99:E217-225, 2014
35. Lapeire L, Hendrix A, Lambein K, Van Bockstal M, Braems G, Van Den Broecke R, Limame R, Mestdagh P, Vandesompele J, Vanhove C, Maynard D, Lehuede C, Muller C, Valet P, Gespach CP, Bracke M, Cocquyt V, Denys H, De Wever O: Cancer-associated adipose tissue promotes breast cancer progression by paracrine oncostatin M and Jak/STAT3 signaling. *Cancer Res* 74:6806-6819, 2014
36. Fadini GP: A reappraisal of the role of circulating (progenitor) cells in the pathobiology of diabetic complications. *Diabetologia* 57:4-15, 2014

Table 1. Characteristics of the study population.

Variable	**Non diabetic (n=21)**	**Type 1 diabetic (n=21)**	**p-value**
Age, years	47.9±2.2	35.4±2.5	<0.001
Male gender, %	52.4	57.2	0.763
Body mass index, kg/m^2	25.3±0.9	24.7±0.6	0.589
Waist circumference, cm	94.2±2.6	89.7±2.0	0.189
Fasting plasma glucose, mg/dl	90.4±1.6	149.8±10.6	<0.001
HbA1c, %	5.5±0.1	7.9±0.2	<0.001
Hypertension, %	23.8	19.0	0.715
Systolic blood pressure, mm Hg	126.4±4.1	121.0±3.5	0.320
Diastolic blood pressure, mm Hg	81.8±2.3	74.3±1.6	0.009
Smoking habit, %	14.3	9.5	0.643
Total cholesterol, mg/dl	196.3±9.6	176.0±7.6	0.102
HDL cholesterol, mg/dl	58.7±3.6	60.2±2.3	0.707
LDL cholesterol mg/dl	112.7±7.8	99.4±5.7	0.171
Triglycerides, mg/dl	124.6±24.5	82.1±9.7	0.101
Retinopathy, %	0.0	33.3	-
Nephropathy, %	0.0	9.5	-
Neuropathy, %	0.0	9.5	-
Atherosclerotic CVD, %	4.7	9.5	0.560
Medications			
Insulin, %	0.0	100.0	-
Metformin, %	0.0	14.2	-
ACE inhibitors, %	19.0	19.0	1.000
Other anti-hypertensives, %	4.8	4.8	1.000
Aspirin, %	23.8	4.8	0.081
Statin, %	61.9	28.6	0.03

FIGURE LEGENDS

Figure 1. Circulating monocyte-macrophages in type 1 diabetic (T1D) patients and controls (CTRL). A) Representative FACS plots illustrating the gates used to identify circulating M1- and M2-like monocyte-macrophages in a CTRL and T1D patient. B) Quantification of the expression of single M1 and M2 markers (left panel) and of M1 and M2 cells (right panel) in CTRL and T1D patients. *p<0.05 T1D vs CTRL. C) Correlations between per cent change in M2 cells and change in $CD34^+$ cells after G-CSF stimulation in CTRL and T1D patients from the NCT01102699 study.

Figure 2. Murine bone marrow macrophage quantification and characterization. A) Representative FACS plots illustrating the gates used to identify BM $Gr\text{-}1^-CD115^-F4/80^+SSC^{low}$ macrophages. The box plot on the right shows quantification of this phenotype in non diabetic (CTRL) and type 1 diabetic (T1D) mice. B) Representative FACS plots illustrating the gates used to identify BM $CD45^+Gr\text{-}1^-MHC\text{-}II^+F4/80^+$ macrophages. The box plot on the right shows quantification of this phenotype in CTRL and T1D mice. C) Representative FACS histograms illustrating the expression of M1 (CD86) and M2 (CD301 and CD206) markers on $Gr\text{-}1^-CD115^-F4/80^+SSC^{low}$ BM macrophages. The graph on the right shows quantification in macrophages from CTRL and T1D mice. D) Gene expression analysis of $Gr\text{-}1^-CD115^-F4/80^+SSC^{low}$ BM macrophages sorted from CTRL and T1D mice. E) FACS histogram (left) and graph (middle) illustrating surface expression of CD169, as well as gene expression (right) on $Gr\text{-}1^-CD115^-F4/80^+SSC^{low}$ BM macrophages of CTRL and T1D mice. *p<0.05.

Figure 3. Effects of bone marrow macrophage depletion. A) Per cent BM macrophages (fold-change versus baseline in controls) in non diabetic (CTRL) and type 1 diabetic (T1D) mice before (baseline) and after a full course of G-CSF stimulation (post G-CSF). *p<0.05 versus baseline or in the comparison indicated by the line. B) Per cent BM macrophages (fold-change versus baseline in

controls) in CTRL and T1D mice before and after macrophage depletion with clodronate liposomes. *p<0.05 versus baseline or in the comparison indicated by the line; n.s., not significant. C) Cxcl12 expression in the whole BM in CTRL and T1D mice before and after macrophage depletion with clodronate liposomes. *p<0.05 versus baseline. D-E) LKS cell (D) and $CD34^{+}Flk\text{-}1^{+}$ cells (endothelial progenitor cells, E) mobilization in CTRL and T1D mice in response to clodronate and clodronate + G-CSF administration in non diabetic and diabetic mice. *p<0.05 versus baseline. #p<0.05 versus clodronate alone.

Figure 4. CD169 expression and CM activity of M1 macrophages. A) Schematic representation of the strategy used for the in silico analysis of CD169 expression in monocytes, M0, M1 and M2 macrophages (GEO dataset GDS2429). B) Average CD169 probe expression in monocytes (Monos), M0, M1 and M2 macrophages from GEO dataset GDS2429 (*p<0.05). C) Representative FACS histograms of surface CD169 expression on in vitro polarization M0, M1, M2 macrophages. D) Gene expression analysis of CD169 expression on cultured M0, M1, M2 macrophages (p<0.05 versus M0). E) Immunofluorescence image indicating Nestin expression on human BM-derived MSCs (left) and effects of M0, M1, M2 macrophage conditioned medium on CXCL12 gene expression by MSCs (*p<0.05 versus CTRL). F) Effects of M0, M1, M2 macrophage CM with or without Proteinase K on CXCL12 expression by MSCs. *p<0.05 versus CTRL. G) Effects of M0, M1, M2 macrophage CM with or without a protease inhibitor on CXCL12 expression by MSCs. *p<0.05 versus CTRL.

Figure 5. Macrophage-derived OSM prevents stem cell mobilization. A) CXCL12 gene expression by MSCs induced by increasing concentrations of OSM (*p<0.05 versus 0). B) OSM protein concentration in M0, M1, and M2 macrophage conditioned media (*p<0.05 versus M0). C) OSM gene expression in cultured M0, M1, M2 macrophages (*p<0.05 versus M0). D) OSM gene expression in the BM as a whole at baseline and after treatment with clodronate liposomes in non

diabetic and diabetic mice (*p<0.05 versus baseline). E) CXCL12 gene expression by MSCs treated with M0, M1 and M2 conditioned media (CM) in the presence or in the absence of an anti-OSM neutralizing antibody (*p<0.05 versus M0). F,G) LKS cell mobilization in response to G-CSF alone (F) or G-CSF + a neutralizing anti-OSM antibody (G) in non diabetic and diabetic mice (*p<0.05 versus baseline). H,K) EPC mobilization in response to G-CSF alone (H) or G-CSF + a neutralizing anti-OSM antibody (K) in non diabetic and diabetic mice (*p<0.05 versus baseline). J) OSM protein concentration in BM plasma of n=6 non diabetic and n=6 diabetic patients (*p<0.05). L) BM-to-PB ratio of $CD34^+$ cells, a surrogate of steady state stem cell mobilization, in non diabetic and diabetic patients (*p<0.05). M) Linear correlation between OSM concentrations and BM-to-PB $CD34^+$ cell ratio.

Figure 6. OSM neutralization improves mobilization and response to ischemia. A) Circulating LKS SC were determined at baseline and 3 days after ischemia in non diabetic mice, diabetic mice and diabetic mice pre-treated with a neutralizing anti-OSM antibody (αOSM). *p<0.05 versus baseline. B) LKS cells were identified by FACS in the cell suspension of ischemic muscles (gastrocnemius and adductors) of non diabetic mice, diabetic mice and diabetic mice pre-treated αOSM. *p<0.05 as indicated. Panels on the right show representative FACS plots of c-kit and Sca-1 staining after gating live ($7AAD^-$) Lin^- events. C) Laser Doppler imaging was used to determine perfusion recovery after ischemia, as the ischemic/non ischemic ratio in the 3 groups of animals. *p<0.05 as indicated. Right panels shown representative laser Doppler images of data quantified in (C).

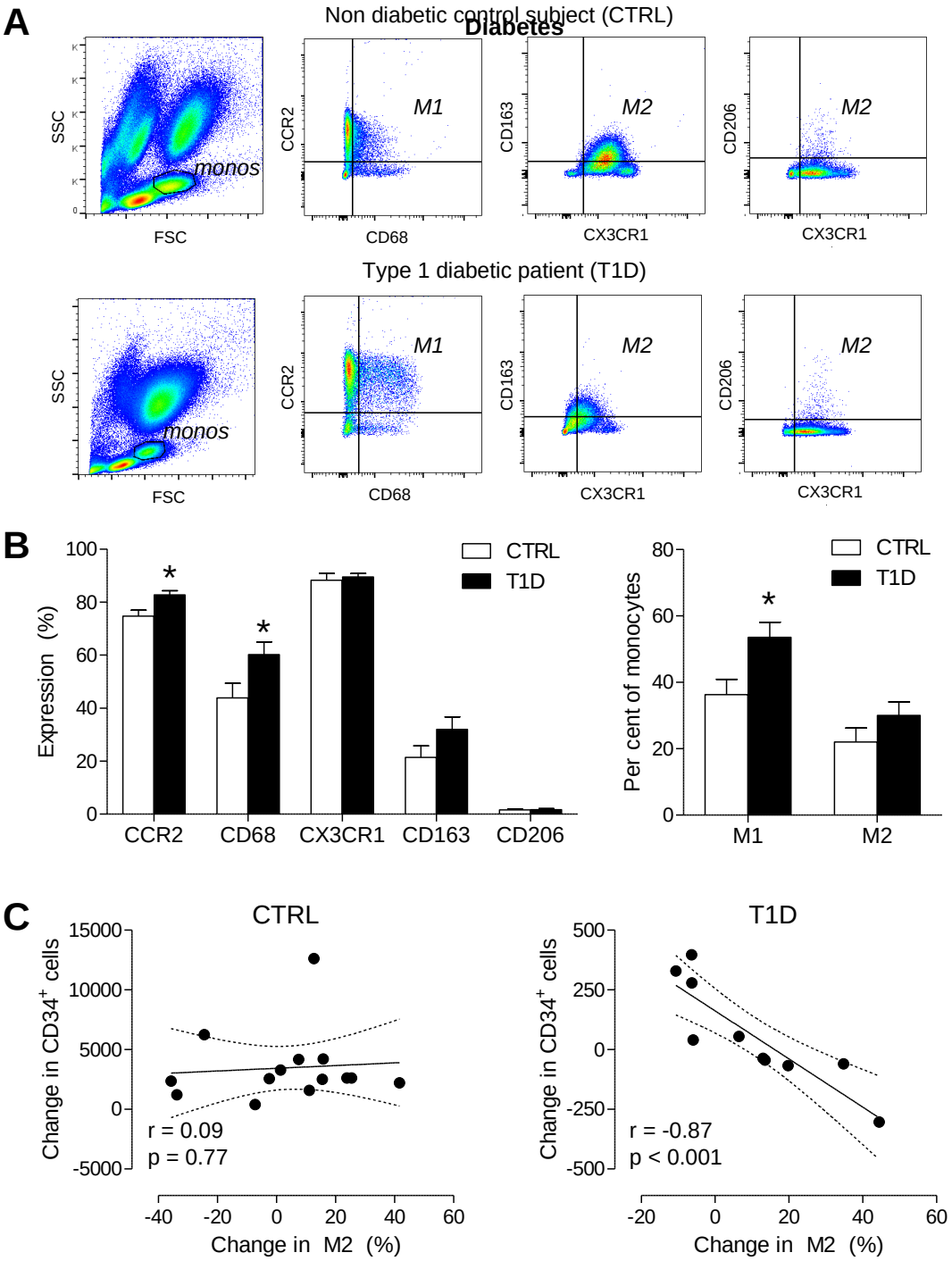
A
Non diabetic control subject (CTRL)
Diabetes
SSC
FSC
monos
CCR2
CD68
M1
CD163
CX3CR1
M2
CD206
CX3CR1
M2
Type 1 diabetic patient (T1D)
SSC
FSC
monos
CCR2
CD68
M1
CD163
CX3CR1
M2
CD206
CX3CR1
M2
B
Expression (%)
CTRL
T1D
CCR2
CD68
CX3CR1
CD163
CD206
Per cent of monocytes
CTRL
T1D
M1
M2
C
CTRL
Change in CD34+ cells
r = 0.09
p = 0.77
Change in M2 (%)
T1D
Change in CD34+ cells
r = -0.87
p < 0.001
Change in M2 (%)

Figure 2

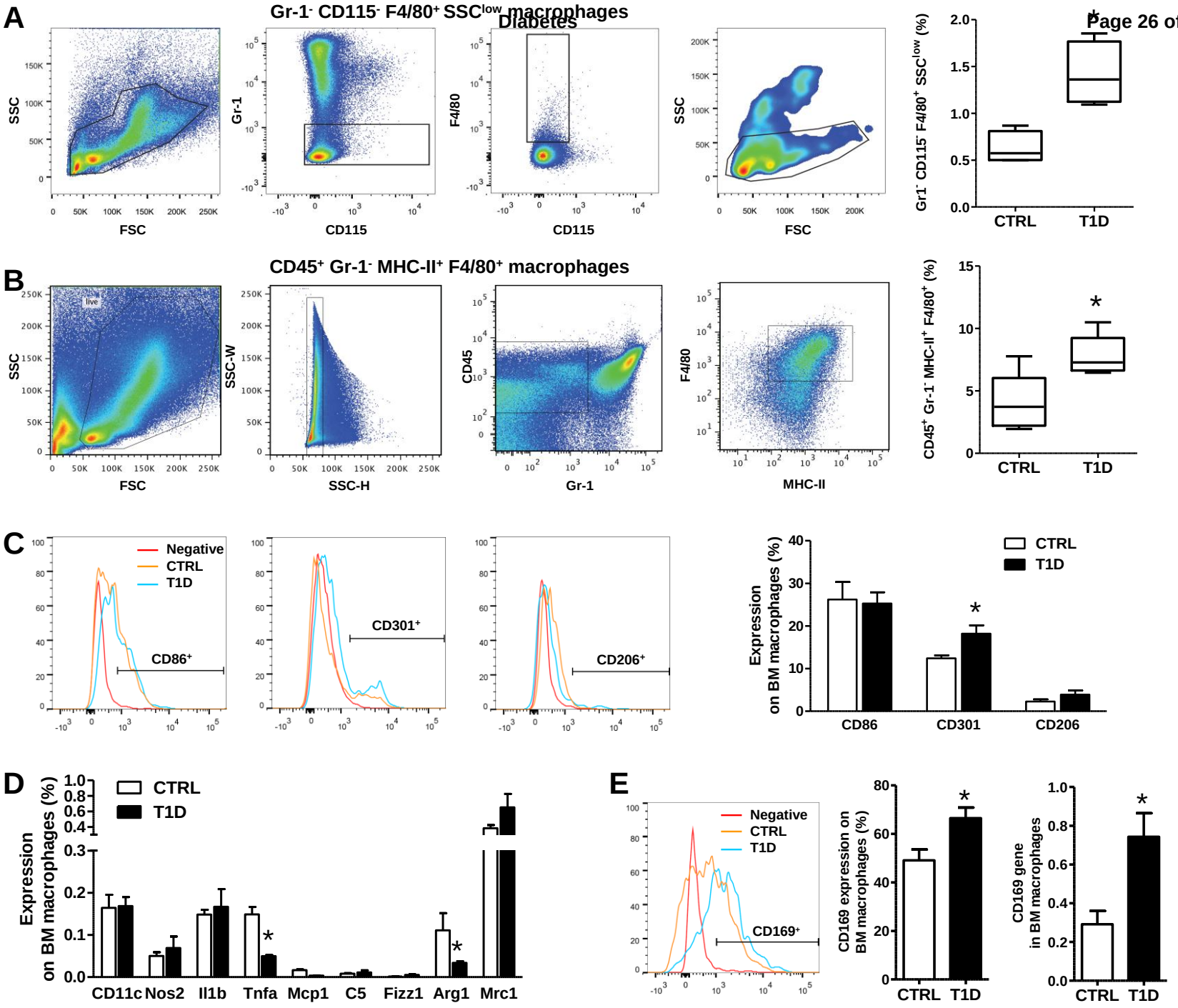
A
Gr-1- CD115- F4/80+ SSClow macrophages
Diabetes
SSC
FSC
Gr-1
CD115
F4/80
CD115
SSC
FSC
Gr1- CD115- F4/80+ SSClow (%)
CTRL
T1D
*
B
CD45+ Gr-1- MHC-II+ F4/80+ macrophages
live
SSC
FSC
SSC-W
SSC-H
CD45
Gr-1
F4/80
MHC-II
CD45+ Gr-1- MHC-II+ F4/80+ (%)
CTRL
T1D
*
C
Negative
CTRL
T1D
CD86+
CD301+
CD206+
Expression on BM macrophages (%)
CTRL
T1D
CD86
CD301
CD206
*
D
CTRL
T1D
Expression on BM macrophages (%)
CD11c
Nos2
Il1b
Tnfa
Mcp1
C5
Fizz1
Arg1
Mrc1
*
*
E
Negative
CTRL
T1D
CD169+
CD169 expression on BM macrophages (%)
CTRL
T1D
*
CD169 gene in BM macrophages
CTRL
T1D
*

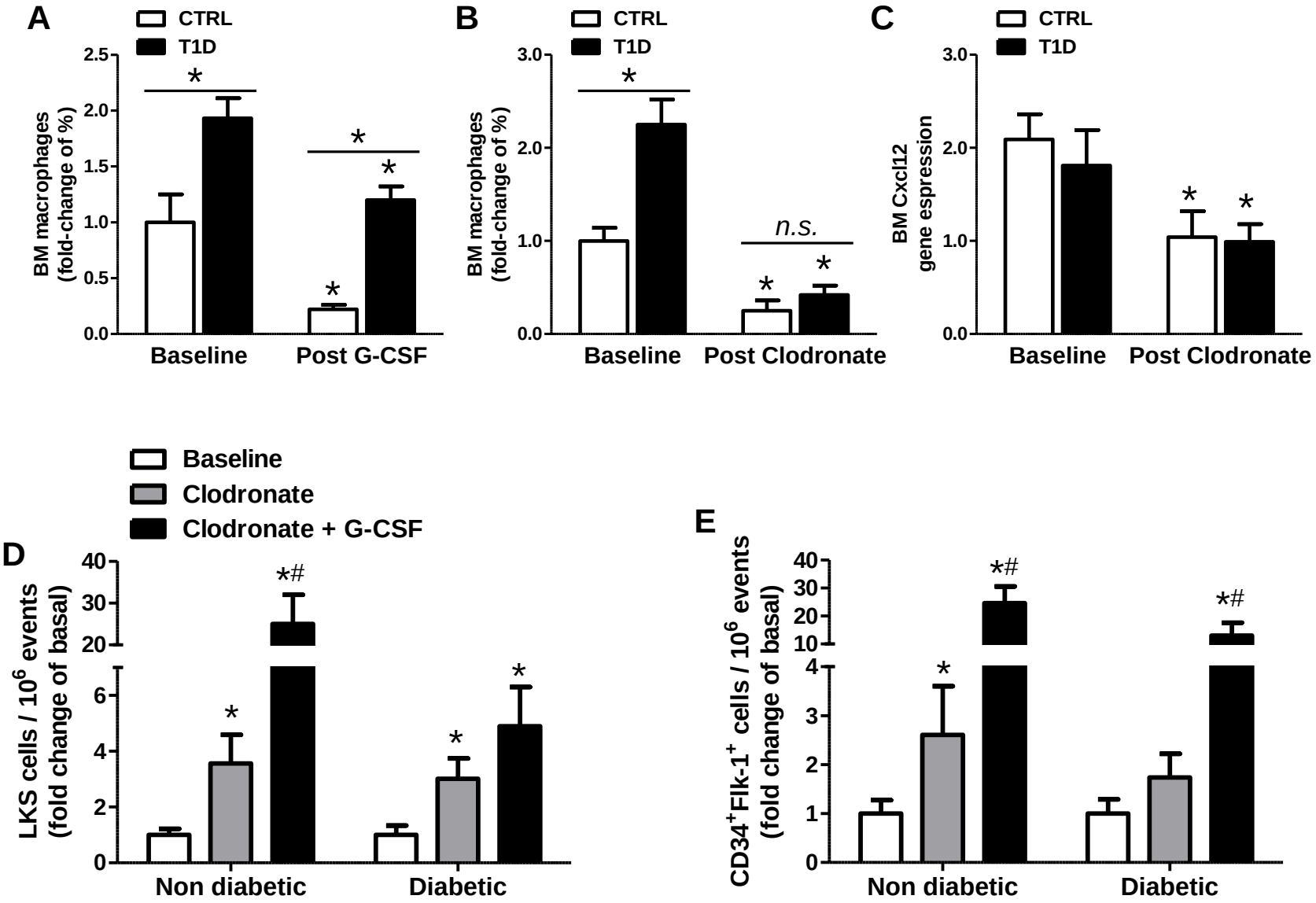
A
CTRL
T1D
BM macrophages (fold-change of %)
2.5
2.0
1.5
1.0
0.5
0.0
*
*
*
*
Baseline
Post G-CSF
B
CTRL
T1D
BM macrophages (fold-change of %)
3.0
2.0
1.0
0.0
*
n.s.
*
*
Baseline
Post Clodronate
C
CTRL
T1D
BM Cxcl12 gene espression
3.0
2.0
1.0
0.0
*
*
Baseline
Post Clodronate
Baseline
Clodronate
Clodronate + G-CSF
D
LKS cells / 10^6 events (fold change of basal)
40
30
20
6
4
2
0
*
*#
*
*
Non diabetic
Diabetic
E
CD34+Flk-1+ cells / 10^6 events (fold change of basal)
40
30
20
10
4
3
2
1
0
*
*#
*
*#
Non diabetic
Diabetic

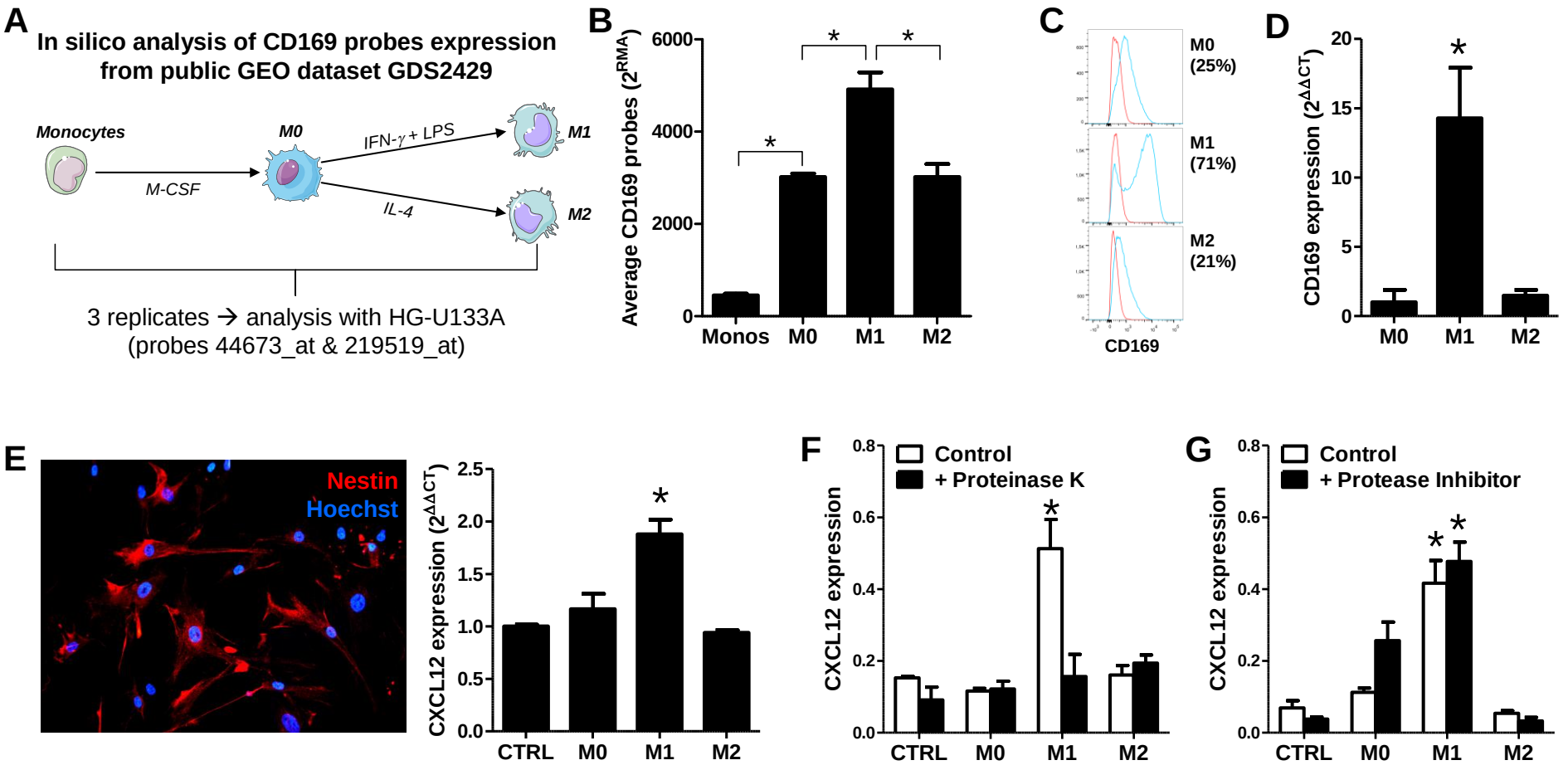
A
In silico analysis of CD169 probes expression from public GEO dataset GDS2429
Monocytes
M-CSF
M0
IFN-γ + LPS
IL-4
M1
M2
3 replicates → analysis with HG-U133A (probes 44673_at & 219519_at)
B
Average CD169 probes (2^RMA)
6000
4000
2000
0
Monos
M0
M1
M2
C
M0 (25%)
M1 (71%)
M2 (21%)
CD169
D
CD169 expression (2^ΔΔCT)
20
15
10
5
0
M0
M1
M2
E
Nestin
Hoechst
CXCL12 expression (2^ΔΔCT)
2.5
2.0
1.5
1.0
0.5
0.0
CTRL
M0
M1
M2
F
Control
+ Proteinase K
CXCL12 expression
0.8
0.6
0.4
0.2
0.0
CTRL
M0
M1
M2
G
Control
+ Protease Inhibitor
CXCL12 expression
0.8
0.6
0.4
0.2
0.0
CTRL
M0
M1
M2

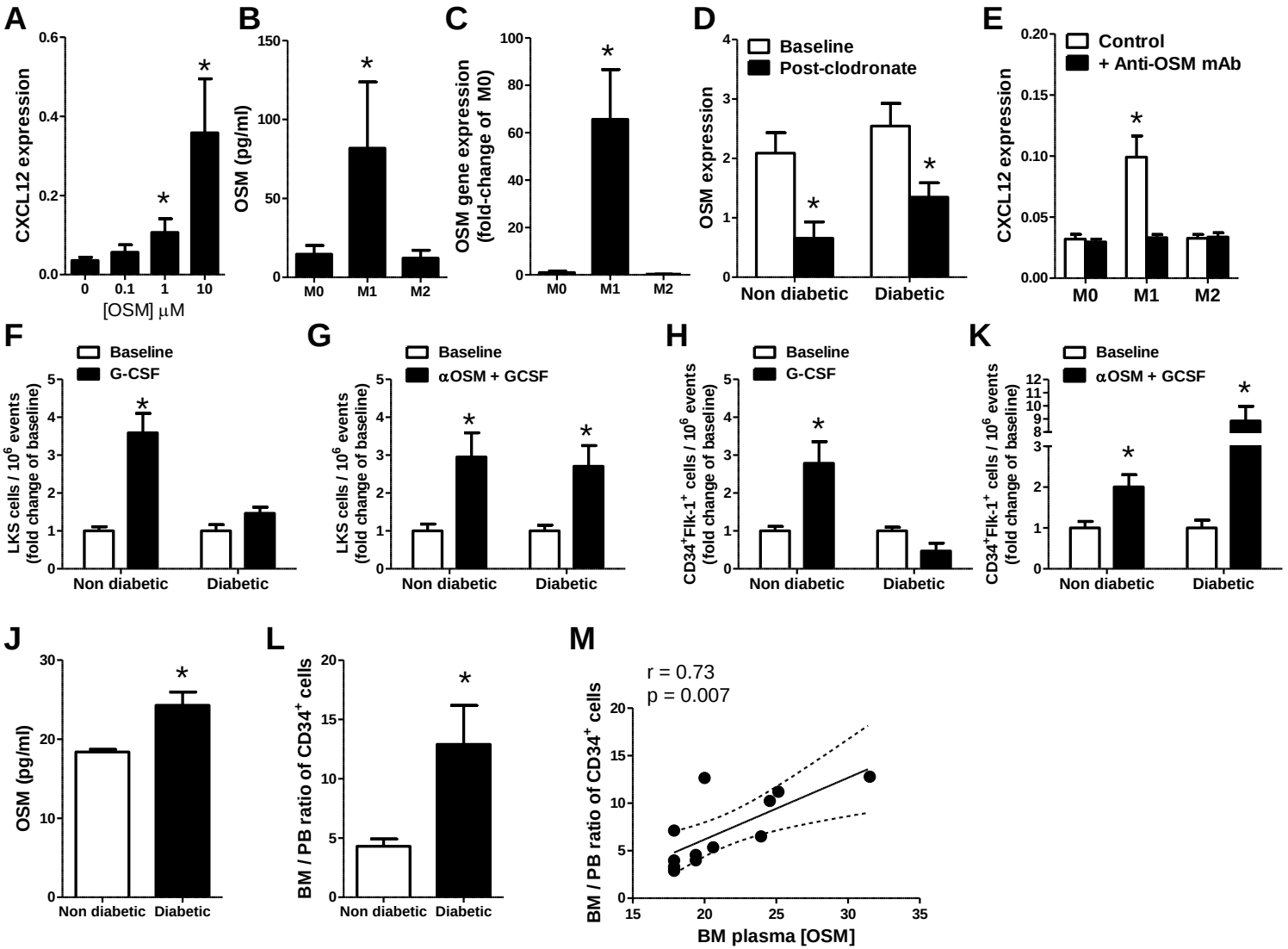
A
CXCL12 expression
0.6
0.4
0.2
0.0
0
0.1
1
10
[OSM] μM
B
OSM (pg/ml)
150
100
50
0
M0
M1
M2
C
OSM gene expression (fold-change of M0)
100
80
60
40
20
0
M0
M1
M2
D
Baseline
Post-clodronate
OSM expression
4
3
2
1
0
Non diabetic
Diabetic
E
Control
+ Anti-OSM mAb
CXCL12 expression
0.20
0.15
0.10
0.05
0.00
M0
M1
M2
F
Baseline
G-CSF
LKS cells / 10^6 events (fold change of baseline)
5
4
3
2
1
0
Non diabetic
Diabetic
G
Baseline
αOSM + GCSF
LKS cells / 10^6 events (fold change of baseline)
5
4
3
2
1
0
Non diabetic
Diabetic
H
Baseline
G-CSF
CD34+Flk-1+ cells / 10^6 events (fold change of baseline)
5
4
3
2
1
0
Non diabetic
Diabetic
K
Baseline
αOSM + GCSF
CD34+Flk-1+ cells / 10^6 events (fold change of baseline)
12
11
10
9
8
3
2
1
0
Non diabetic
Diabetic
J
OSM (pg/ml)
30
20
10
0
Non diabetic
Diabetic
L
BM / PB ratio of CD34+ cells
20
15
10
5
0
Non diabetic
Diabetic
M
r = 0.73
p = 0.007
BM / PB ratio of CD34+ cells
20
15
10
5
0
15
20
25
30
35
BM plasma [OSM]

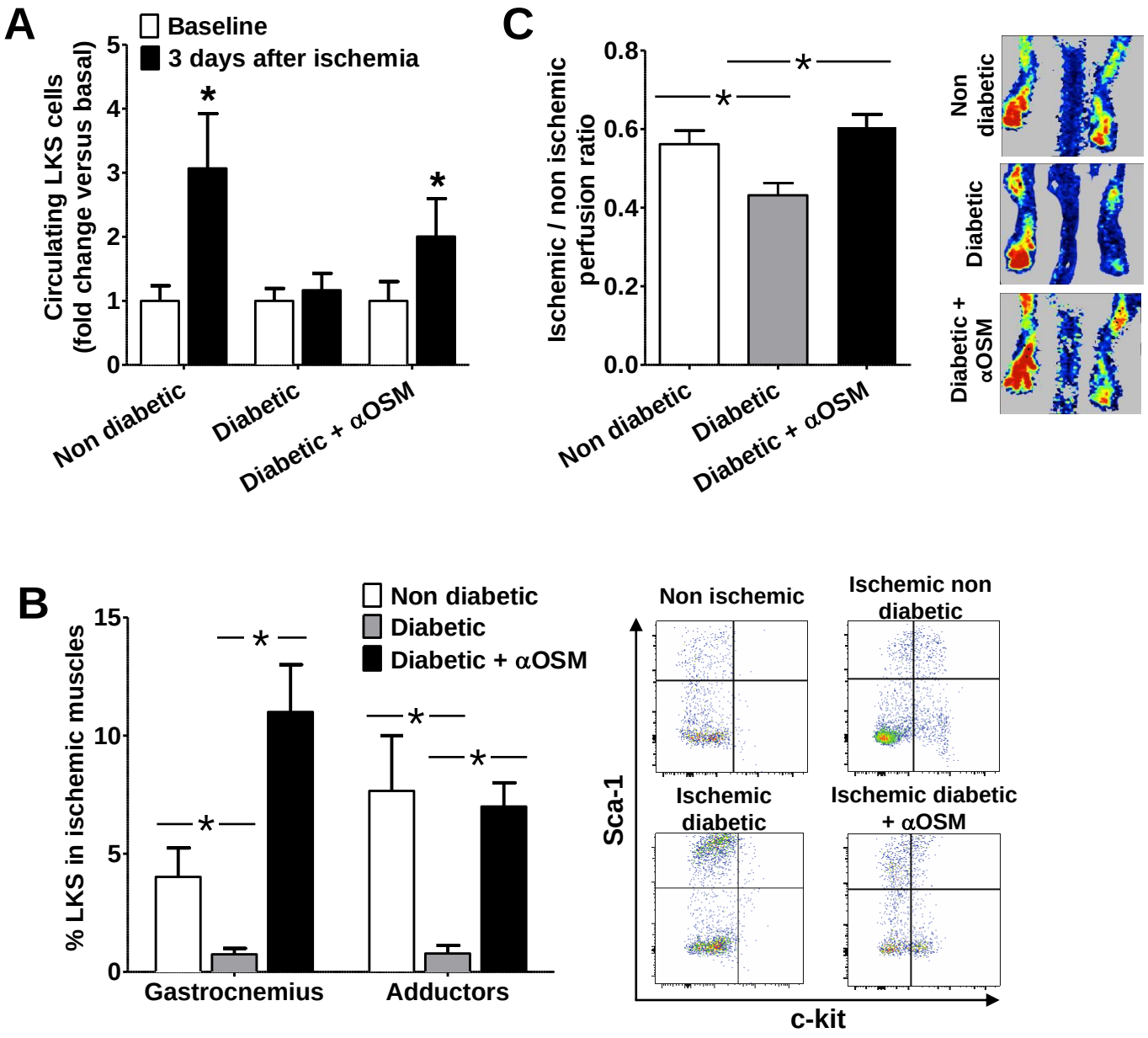
A
Baseline
3 days after ischemia
Circulating LKS cells (fold change versus basal)
0
1
2
3
4
5
*
*
Non diabetic
Diabetic
Diabetic + αOSM
C
Ischemic / non ischemic perfusion ratio
0.0
0.2
0.4
0.6
0.8
*
*
Non diabetic
Diabetic
Diabetic + αOSM
Non diabetic
Diabetic
Diabetic + αOSM
B
Non diabetic
Diabetic
Diabetic + αOSM
% LKS in ischemic muscles
0
5
10
15
*
*
*
*
Gastrocnemius
Adductors
Non ischemic
Ischemic non diabetic
Ischemic diabetic
Ischemic diabetic + αOSM
Sca-1
c-kit

Albiero et al.

Bone marrow macrophages contribute to diabetic stem cell mobilopathy by producing Oncostatin M

ONLINE DATA SUPPLEMENT

Additional details on patients recruitment and characterization. Subjects were enrolled provided they were free from any acute disease or infection and did not report active inflammatory conditions (e.g. rheumatic diseases), recent trauma or surgery, pregnancy/lactation. The following data were collected for all participants: age, sex, body mass index, history of hypertension, smoking habit, prevalence of cardiovascular disease, and medications. We also collected a fasting blood sample for determination of HbA1c and lipid profile, and a spot urinary sample for determination of albumin/creatinine ratio (ACR). Coronary artery disease (CAD) was defined as a past history of myocardial infarction or angina, or angiographic evidence of >50% obstruction of epicardial coronary arteries, or a positive myocardial perfusion stress test. Peripheral arterial disease (PAD) was defined in the presence of claudication or rest pain, or evidence of >50% obstruction in lower extremity arteries or an ankle-brachial index of less than 0.9. Cerebrovascular disease (CerVD) was defined as a past history of stroke or transient ischemic attack, or evidence of >30% carotid artery stenosis, or carotid endarterectomy. Prevalent atherosclerotic cardiovascular disease (CVD) was defined as either CAD, or PAD or CerVD isolated or in combination. In diabetic patients, we also recorded disease duration, prevalence of retinopathy (defined by digital funduscopic examination), neuropathy (defined by typical signs and symptoms, eventually confirmed by vibration perceptive threshold and/or electromyography), and nephropathy (defined as an albumin excretion rate >30 mg/g creatinine and/or estimated glomerular filtration rate <60 ml/min/1.73 m^2).

Additional details on animal protocols. Diabetes was induced with a single i.p. injection of 150 mg/kg STZ (Sigma Aldrich, St.Louis, MO, USA) in citrate buffer 50 mM, ph 4.5. Blood glucose was measured with Glucocard G-meter (Menarini, Florence, Italy); animals with blood glucose ≥300 mg/dl in at least two measurements within the first week were classified as diabetic and housed for 4 weeks with feeding and drinking ad libitum before performing experiments. Vav1-$Sirt1^{-/-}$ mice have been described previously (1). For SNS disruption, animals received intraperitoneal injections 100 mg/kg 6-hydroxy-dopamine (6-OHDA, Tocris Bioscience, Bristol, UK), as previously described (1).
Hind limb ischemia. Animals were sedated with 10 mg/kg zolazepam/thylamine (Zoletil®, Laboratories Virbac, Nice, France) and 7 mg/kg xylazine (Xilor®, Laboratories Carlier, Spain). The femoral artery and the vein were surgically dissected from the femoral nerve, then cauterized with low temperature cautery and excised between inguinal ligament and hackle. Stem/progenitor cell mobilization was assessed after 3 days, whereas we measured hind limb microvascular perfusion with Perimed Periscan-Pim II Laser Doppler System (Perimed AB, Sweden) and collected the limb muscles for analysis 14 days after surgery. In a separate batch of experiments (n≥3/group), animals were pretreated with the anti-OSM neutralizing antibody (αOSM) 24h before induction of ischemia.

Additional details on reagents. Antibodies. Monoclonal anti-mouse Ly-6G (Gr-1) PE (clone RB6-8C5, eBioscience, San Diego, CA, USA); monoclonal anti-mouse CD115 Alexa Fluor® 488 (clone AFS98, eBioscience); monoclonal anti-mouse F4/80 APC (clone BM8, eBioscience); monoclonal anti-human CD169 APC (clone 7-239, eBioscience); rat anti-mouse CD169 (clone MOMA-1, AbD Serotec, Oxford, UK). Citokines. Recombinant human Oncostatin M ; Recombinant human TNF-a;

Recombinant human IL-6; Recombinant human RANTES; Recombinant human CXCL10; Recombinant human PDGF-AA; Recombinant human IL-4; Recombinant human IL-13; Recombinant human INF gamma; Recombinant human IL-15 all by PeproTech (Rocky Hill, NJ, USA). Recombinant human LIF Recombinant murine IL-4; Recombinant IL-13 and Recombinant INF-gamma were by Miltenyi Biotec (Cologne, Germany).

Additional details on mobilization assays. G-CSF stimulation. Progenitor cell levels were quantified in peripheral blood after peripheral ischemia or after 4 days of s.c. injection of 200 μg/kg/die of hrG-CSF (Filgrastim, Roche, Basel, Switzerland). BM macrophage depletion. Clodronate liposomes were used to deplete BM macrophages and induce mobilization: 250 ul of clodronate liposome (ClodronateLiposomes.com, The Netherlands) were injected intravenously. Flow cytometry was performed on blood collected at basal and 24 hours after liposome administration. In separate experiments, clodronate liposomes were given 24 hours before beginning G-CSF administration as described above. Oncostatin M neutralization. The day before starting G-CSF stimulation, 100 μg of an anti-OSM antibody (AF-495-NA, R&D Systems) were injected intraperitoneally in diabetic and non diabetic mice.

Additional details on FACS analysis. Human samples. Circulating monocyte-macrophages were identified and quantified as previously described. Briefly, after red blood cell lysis, cells stained with FITC-conjugated anti-CD68 mAb (Dako) and PE-conjugated anti-CCR2 mAb (R&D Systems) for identification of M1 cells and with FITC-conjugated anti-CX3CR1 (Biolegend), PE-conjugated anti-CD163 (BD) and APC-conjugated anti-CD206 (BD) mAbs for M2. M1 were defined as $CD68^{+}CCR2^{+}$ cells and M2 were defined as $CX3CR1^{+}CD163^{+}/CD206^{+}$. Baseline and post-G-CSF levels of circulating $CD34^{+}$ stem cells were quantified as previously described (2).
Murine samples. For identification of murine BM macrophage phenotypes we used the protocol described by Chow et al. (3). Cells were isolated by flushing femurs and tibia. After red blood cell lysis, cells were stained with Gr-1 (Ly6C/G, eBiosciences), CD115 (eBiosciences), and F4/80 (eBiosciences). Macrophages were identified in the $Gr\text{-}1^{neg}/CD115^{neg}$ gate as cells expressing the macrophage marker F4/80 with low side scatter, to distinguish them from eosinophils. $Gr\text{-}1^{+}CD115^{-}$ neutrophils, $Gr\text{-}1^{high}CD115^{+}$ monocytes and $Gr\text{-}1^{-}CD115^{+}$ monocytes were also identified, scored and sorted, when needed for gene expression analyses, using a BD FACS-Aria instrument. In parallel experiments, macrophages were also identified as cells that co-expressed F4/80 and MHC-II (eBiosciences) in the $CD45^{+}Gr\text{-}1^{-}$ gate.
Progenitor cell levels were quantified in peripheral blood after peripheral ischemia (at day 3) or after 4 days of s.c. injection of 200 μg/kg/die of hrG-CSF (Filgrastim, Roche, Basel, Switzerland). 150 μl of peripheral blood were stained with rat anti-mouse APC-lineage cocktail (BD, NJ, USA), PE rat anti-mouse Sca-1 (Ly6A/E, BD) and FITC rat anti-mouse cKit (BD) to quantify LKS cells or with Alexa647 rat anti-mouse CD34 (BD) and Alexa488 anti-mouse Flk-1 (Biolegend, San Diego, CA, USA) to quantify endothelial-committed progenitors. A total of 250.000 events were acquired for each analysis and the level of progenitor cells was expressed as number of positive events per 1.000.000 total events. Data were acquired using a FACS Calibur instrument (BD Biosciences) and analyzed with FlowJo X (TreeStar Inc., USA). For identifying LKS cells in the ischemic muscles, the tissue was digested with collagenase and the cell suspension was analyzed by FACS: singlet, live (7-AAD negative) cells were gated for negative lineage markers and Sca-1 / c-kit expression as described above.

Additional data on cell culture. Human monocyte-derived macrophages. Venous blood was obtained from healthy donors and separated using a Ficoll-Paque solution (Sigma Aldrich). Mononuclear cells were collected, washed with PBS containing EDTA (5 mmol/L) and resuspended at 2×10^{6} cells/mL in RPMI-1640 supplemented with 2 mmol/L glutamine, 0.5% penicillin-streptomycin and 15% FCS. Monocytes were separated from lymphocytes by adherence

to 100-mm plastic dishes for 2 hours at 37°C, 5% CO_2. Adherent monocytes were cultured in fresh medium for 7 days at 37°C to allow spontaneous differentiation into macrophages. At the end of the differentiation period, resting cells were polarized into M1 or M2 macrophages by 48h incubation with LPS (1 μg/ml) and IFN-γ (10 ng/ml) or IL-4 (20 ng/ml) and IL-13 (5 ng/ml), respectively.
Generation of conditioned medium. After 48 hours polarization, the medium was removed. Macrophages were thoroughly washed with PBS and kept in serum-free RPMI for further 72 hours. Afterwards macrophage conditioned media (CM) were harvested, centrifuged at 4000 x g for 20 min, passed through a 0.22-μm filter to eliminate the cellular debris and then stored at -20 °C. For in vitro experiments, CM from M0, M1 and M2 macrophages were concentrated 10-fold using Centriplus filters with 3 kDa cut-off (Amicon) and used at 20% v/v.
Human bone marrow MSCs were obtain from the BM of patients undergoing orthopedic surgery at the University Hospital of Padova (Ethical Committee prot. n. 2868P). Aspirates were washed twice with ice-cold sterile PBS and the cell pellets were plated on TC Petri dishes (Beckton Dickinson) with complete mesenchymal medium (MesenCult plus Mesenchymal Stem Cell Stimulatory Supplements, Stem Cells technologies Inc.). The medium was changed when fibroblast-like cells began to appear and then every other day. Experiments were performed with MCS at passage 5 or lower.
Murine MSCs. MSC were obtained by from 3 months old male wild-type C56Bl6/J mice from in-house colony. Mice were euthanized and femurs and tibia removed. Under sterile condition, bones were carefully cleaned from tissue debris and flushed with ice cold PBS. Cells were plated on TC Petri dishes (BD) with MEM-alpha medium (Sigma Aldrich) supplemented with glutamine, penicillin-streptomycin and 15% FBS, until cells reached 70% confluence and then passed for expansion. For experiments, mMSC were used up to passage 6. Murine macrophages. Mouse BMM were obtained by flushing with sterile ice-cold PBS both femurs and tibia of 3 months old male wild-type C56Bl6/J mice. Red blood cells were lysed with Ammonium-Chloride-Potassium Lysing Buffer. To obtain resting macrophages, 150.000 cells/cm^2 were plated on tissue culture Petri dishes with RPMI-1640 medium supplemented with glutamine, penicillin-streptomycin and 10% FCS + 10 nM murine macrophage-colony stimulating factor (M-CSF, Miltenyi Biotech) for 7 days without any medium change. Thereafter, macrophages were polarized toward M1 or M2 phenotype by incubation for 48 h with lipopolysaccharide (LPS; 1 μg/ml) and IFN-γ (10 ng/ml) or IL-4 (20 ng/ml) and IL-13 (5 ng/ml), respectively. Medium was then changed with RPMI-1640 medium supplemented with glutamine, penicillin-streptomycin without serum for 48 hours to yield conditioned medium. For each batch of conditioned medium, at the end of the experiments BMM were collected and analyzed by flow cytometry or kept in Trizol® for gene expression analysis.
In addition to MSCs, in some experiments, HUVECs, HAECs and human fibroblasts were used to study the effects of OSM on CXCL12 expression. Previously described standard protocols were used to culture humans fibroblasts (4), HUVECs and HAECs (5).
Permeability assay. Permeability of an endothelial cell monolayer was evaluated using HUVECs grown at confluence on fibronectin according to the vascular permeability assay as described by Ma et al (6).

Technical details of gene expression analyses. Total RNA was extracted using Trizol® reagent and following the manufacturer's protocol. RNA quantity was determined by a Nanodrop Spectrometer (Thermo-Fisher Scientific Inc) (using 1 OD260 = 40μg RNA). A260/A280 ratios were also calculated for each sample. RNA was then reverse transcribed to generate cDNA using the First-Strand cDNA Synthesis Kit from Invitrogen® following the protocol provided by the manufacturer. Reverse Transcription was performed using 400 ng of RNA with the following reaction mix: 250 ng of random primers, 1 μl 10 mM dNTP Mix (10 mM each dATP, dGTP, dCTP and dTTP at neutral pH) and sterile, distilled water to 13 μl. The sample were mixed by vortexing, briefly centrifuged and denaturated by incubation for 5 minutes at 70°C to prevent secondary structures of RNA. Samples were incubated on ice for 2 minutes to allow the primers to align to the

RNA and the following components were added sequentially: 4 µl 5X First-Strand Buffer, 1 µl 0.1 M DTT, 1 µl RNaseOUT™ Recombinant RNase Inhibitor, 1 µl of SuperScript™ III RT (200 units/µl), all by Invitrogen. At the end of reaction, the volume of each sample was adjusted to 40 µl with RNase free water. Duplicates of sample cDNA were then amplified on the 7900HT Fast Real-Time PCR System (Applied Biosystems) using the Fast SYBR Green RT-PCR kit (Applied Biosystems) in 96-wells or 384-wells plates (Micro Amp Optical, Applied Biosystems) by adding: 4.8 µl of Fast SYBR Green master Mix, 0.2 µl Primer Mix (15 µM), 5.0 µl of diluted cDNA. Specificity of gene amplification was confirmed by analyzing the dissociation curve with SDS 2.3 software (Applied Biosystems). Expression data were normalized to the mean of housekeeping gene ubiquitin C to control the variability in expression levels and were analyzed using the 2(-ΔΔCT) method. Gene-specific primer pairs were designed using Primer-BLAST (NCBI) and were each validated prior to use by gradient PCR and gel analysis to test for optimal annealing temperature, reaction efficiency and specificity (Table S1).

Additional data on in vitro CXCL12 assays. Human and mouse MSC were plated on 6-well TC plates (BD) for each experiment. Upon reaching 90% confluence, cytokines and chemicals was added at given concentrations with Mesencult medium without supplements. Conditioned media were incubated with anti-Oncostatin M antibodies, mouse anti-human and rabbit anti-mouse (MAB295 and AF-495-NA respectively; R&D), at 37°C for 30 minutes and then added to the cells. Macrophage conditioned media were treated with 0.5 mg/ml proteinase K (Sigma-Aldrich, St. Louis, MO) for 30 min at 37°C and then heat inactivated at 95°C for 10 min and then added to MSC for 48 hours. All experiments were conducted for 48 hours and then cells were lysed with Trizol for gene expression analysis. For STAT3 phosphorylation experiments, we used Phosphoflow® PE Mouse Anti-Stat3 (pY705, BD) according to the manufacture's instruction.
CXCL12 protein was measured using the R&D Systems (DSA00 for human and MCX120 for mouse). OSM protein was quantified by ELISA (Raybiotech ELH-OSM for human; R&D MSM00 for mouse). To explore the pathways mediating effects of OSM on CXCL12 expression, we used the following chemicals. Inhibitors of p38 (SB202190), STAT3 (Stattic, S7024), JNK (SP600125), ERK 1/2 (SCH 772984) were from Selleckchem (Houston, TX, USA). Inhibitor of MEK (U0126) from Calbiochem, Millipore. Amlexanox (NF-kB inhibitor), colivelin and anisomycin were from Tocris (R&D Systems), protease inhibitor (P1860) and Pi3K inhibitor (Wortmannin) were from Sigma Aldrich.
Murine bone marrow sample were obtained by pulverizing 1 femur with liquid nitrogen and by adding 250 ul of ice-cold PBS with complete protease inhibitor cocktail (Roche, Basel, Switzerland). After orbital rotation at 4°C for 15 minutes, samples were centrifuged at 13300 RPM at 4°C and surnatants kept at -80°C for analysis.

Specific details of the in silico analyses. In silico analyses were performed retrieving data from GEO database. GSE32690 dataset was used to get murine expression data, and in particular we analyzed the following groups of samples: GSM812310, GSM812311, GSM812312 (M(-)); GSM812313, GSM812314, GSM812315 (M(IFNγ+LPS)); GSM812316, GSM812317; GSM812318 (M(IL-4)). GSE5099 dataset was used to get human expression data, grouped as follows: GSM115052, GSM115053, GSM115054, GSM115067; GSM115068, GSM115069 (M(-));GSM115055, GSM115056, GSM115057, GSM115070, GSM115071, GSM115072 (M(IFNγ+LPS)); GSM115058, GSM115059, GSM115060, GSM115073, GSM115074, GSM115075 (M(IL4)). Murine and human expression data were both divided in two different groups (M(-) or M0 vs M(IFNγ+LPS) or M1 and M(IL4) or M2 vs M(IFNγ+LPS) or M1, and then analyzed using GEO2R tool, selecting the Benjamini & Hochberg false discovery rate p-value adjustment. We subsequently filtered data according to these stringent criteria: being upregulated in M(IFNγ+LPS) verus M(-) and versus M(IL4) macrophages at least 5 folds (logFC>2.32), and with an adjusted p-value <0.001, in both groups. The two groups where then crossed, to get a list of

genes commonly upregulated in M(IFNγ+LPS) macrophages. Since we were interested in secreted proteins, data were furthermore filtered by comparing the previous human and murine gene lists respectively with a specie-specific secreted protein list. These were obtained from the Metazoa Secretome and Subcellular Proteome Knowledgebase (MetazSecKB, http://proteomics.ysu.edu/secretomes/animal/index.php), choosing the "Curated secreted" option for both human and murine list, after converting each of them from UniProt accession to official gene name with David conversion tool (http://david.abcc.ncifcrf.gov/conversion.jsp). We manually checked for proteins which have a known receptor. Finally, we compared this list with microarray expression data of human (GSM139891, GSM139892, GSM139893, GSM139907, GSM139908, GSM139909, part of GSE6029) and murine (GSM1071218, GSM1071219, GSM1071220, part of GSE43781) bone marrow derived mesenchymal stem cells, to check whether these receptors were expressed at any level.

References

1. Albiero M, Poncina N, Tjwa M, Ciciliot S, Menegazzo L, Ceolotto G, Vigili de Kreutzenberg S, Moura R, Giorgio M, Pelicci P, Avogaro A, Fadini GP: Diabetes causes bone marrow autonomic neuropathy and impairs stem cell mobilization via dysregulated p66Shc and Sirt1. *Diabetes* 63:1353-1365, 2014

2. Fadini GP, Albiero M, Vigili de Kreutzenberg S, Boscaro E, Cappellari R, Marescotti M, Poncina N, Agostini C, Avogaro A: Diabetes impairs stem cell and proangiogenic cell mobilization in humans. *Diabetes Care* 36:943-949, 2013

3. Chow A, Lucas D, Hidalgo A, Mendez-Ferrer S, Hashimoto D, Scheiermann C, Battista M, Leboeuf M, Prophete C, van Rooijen N, Tanaka M, Merad M, Frenette PS: Bone marrow CD169+ macrophages promote the retention of hematopoietic stem and progenitor cells in the mesenchymal stem cell niche. *J Exp Med* 208:261-271, 2011

4. Ceolotto G, Papparella I, Lenzini L, Sartori M, Mazzoni M, Iori E, Franco L, Gallo A, de Kreutzenberg SV, Tiengo A, Pessina AC, Avogaro A, Semplicini A: Insulin generates free radicals in human fibroblasts ex vivo by a protein kinase C-dependent mechanism, which is inhibited by pravastatin. *Free Radic Biol Med* 41:473-483, 2006

5. Albiero M, Rattazzi M, Menegazzo L, Boscaro E, Cappellari R, Pagnin E, Bertacco E, Poncina N, Dyar K, Ciciliot S, Iwabuchi K, Millioni R, Arrigoni G, Kraenkel N, Landmesser U, Agostini C, Avogaro A, Fadini GP: Myeloid calcifying cells promote atherosclerotic calcification via paracrine activity and allograft inflammatory factor-1 overexpression. *Basic Res Cardiol* 108:368, 2013

6. Ma C, Wang XF: In vitro assays for the extracellular matrix protein-regulated extravasation process. *CSH Protoc* 2008:pdb prot5034, 2008

Table S1. Primer sequences (m, mouse; h, human).

Gene	FW primer sequence	Rv primer sequence
m CD169	AAGTGTGCTGTATGCCCCAG	GGAACAGAGACAGGTGAGCC
m CD11c	TCTTCTGCTGTTGGGGTTTGT	GAGCACACTGTGTCCGAACT
m Cxcl12	GAGCCAACGTCAAGCATCTG	CGGGTCAATGCACACTTGTC
m nos2	TCCTGGACATTACGACCCCT	CTCTGAGGGCTGACACAAGG
m Tnfα	GTGGAACTGGCAGAAGAG	CCATAGAACTGATGAGAGG
m mrc1	TTGCACTTTGAGGGAAGCGA	CCTTGCCTGATGCCAGGTTA
m C5	CAGGGTACTTTGCCTGCTGA	TGGATTTTCATGGTGGGGCA
m Arg	ACAAGACAGGGCTCCTTTCAG	GGCTTATGGTTACCCTCCCG
m Mcp1	AGCTGTAGTTTTTGTCACCAAGC	GTGCTGAAGACCTTAGGGCA
h CD206	CCTCTGGTGAACGGAATGAT	AGGCCAGCACCCGTTAAAAT
h IL10	TACGGCGCTGTCATCGATTT	TGAGAGTCGCCACCCTGATGT
h IL1BETA	AACCTCTTCGAGGCACAAGG	GTCCTGGAAGGAGCACTTCAT
h CD169	TCGACGCTCAAGCTGTGAAT	CCATGTGTAGGTGAGCTGGG
h VCAM	GTTTGCAGCTTCTCAAGCTTTT	GATGTGGTCCCCTCATTCGT
h ANGPT	CAGACTGCAGAGCAGACCAGAA	CTCTAGCTTGTAGGTGGATAATGAATTC
h KITL	CGGGATGGATGTTTTGCCAAG	TTTCACGCACTCCACAAGGT
h CXCL12	ATGCCCATGCCGATTCTT	GCCGGGCTACAATCTGAAGG
h β-ACTIN	AGAGCTACGAGCTGCCTGAC	GGATGCCACAGGACTCCA

Table S2. Characteristics of patients in the BM sub-study.

Variable	Non diabetic (n=6)	Diabetic (n=6)	p-value
Age, years	60.8±5.6	65.8±4.0	0.484
Sex male, %	83.3	100.0	0.340
Body mass index, kg/m1	24.5±1.5	29.0±2.0	0.161
Fasting plasma glucose, mg/dl	91.5±6.6	220.0±51.0	0.032
Hypertension, %	66.6	100.0	0.145
Systolic blood pressure, mm Hg	127.7±9.1	126.5±14.8	0.947
Diastolic blood pressure, mm Hg	64.7±4.1	75.7±6.8	0.197
Smoking habit, %	33.3	0.0	0.145
Total cholesterol, mg/dl	178.5±10.8	143.2±8.2	0.026
HDL cholesterol, mg/dl	51.3±5.0	40.8±4.1	0.134
LDL cholesterol mg/dl	109.3±13.9	72.2±7.5	0.040
Triglycerides, mg/dl	90.0±9.7	152.8±26.2	0.048
Medications			
Insulin, %	-	33.3	-
Oral antidiabetic agents, %	-	50.0	-
ACE inhibitors, %	100.0	83.3	0.340
Aspirin, %	83.3	83.3	1.000
Statin, %	50.0	66.6	0.599

SUPPLEMENTAL FIGURES

Supplemental figure 1. A) Percentages of BM macrophages in control (CTRL) and sympathectomised mice treated with 6-OHDA. B) Percentages of BM macrophages in CTRL and hematopoietic (Vav-driven) Sirtuin-1 (Sirt1) knockout mice.

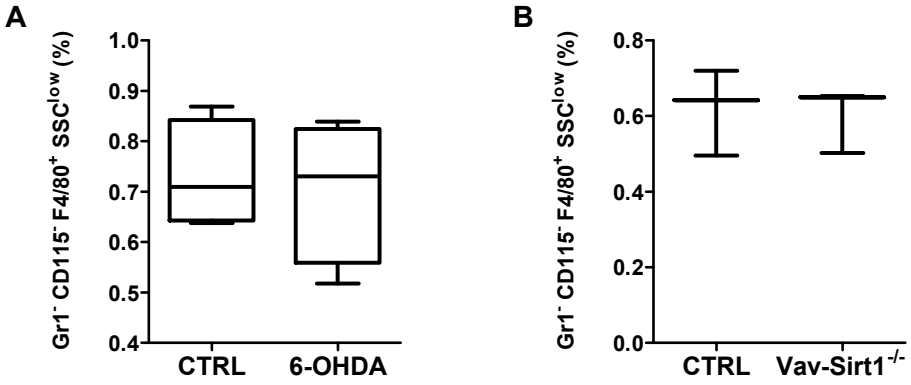

Supplemental figure 2. Surface expression of CD169 was analyzed by FACS in BM cell populations identify by Gr-1, CD115 and F4/80 staining. Identity of the gated populations was confirmed by Hoechst nuclear staining morphology of sorted cells. The FACS histogram shows that CD169 is expressed at higher levels in macrophages compared to other populations.

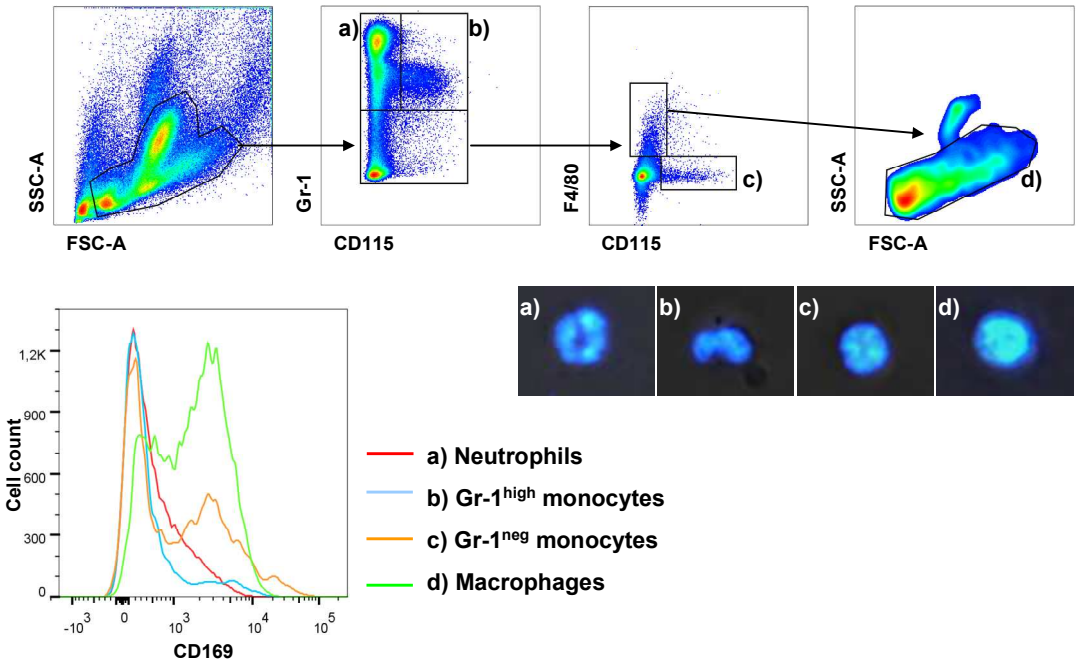

Supplemental figure 3. A) Changes in PB Gr-1^{-}CD115^{-}F4/80^{+}SSC^{low} macrophages, BM Gr-1^{high} and Gr-1^{low} monocytes, as well as neutrophils after clodronate liposome treatment compared to baseline in non diabetic (CTRL) and type 1 diabetic (T1D) mice. B) Changes in niche gene expression in the whole BM after clodronate liposome treatment compared to baseline in CTRL and T1D mice. *p<0.05 versus baseline.

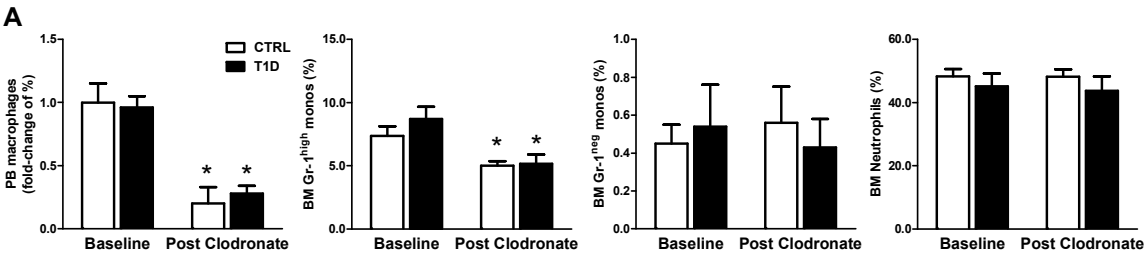

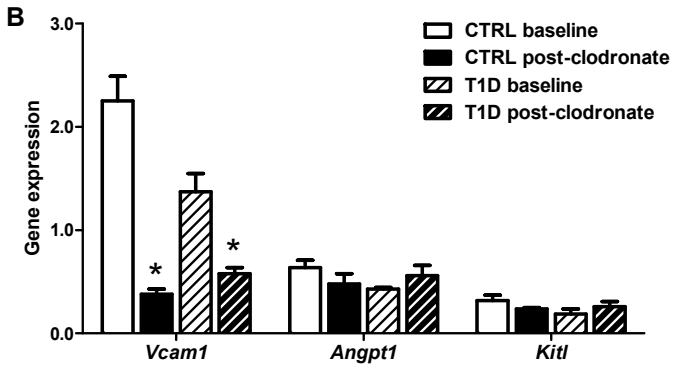

Supplemental figure 4. Expression of typical M1 and M2 genes in cultured polarized macrophages, relative to expression in resting M0. *p<0.05 M1 versus M2.

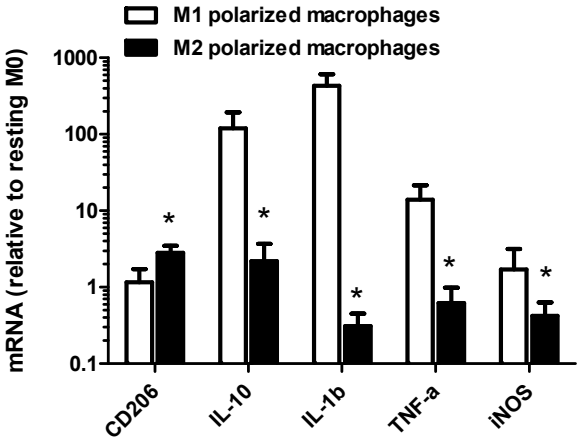

Supplemental figure 5. Changes in the expression of niche genes in MSCs in the control condition (CTRL) or incubated with M0, M1 and M2 macrophage conditioned media. *p<0.05 versus CTRL.

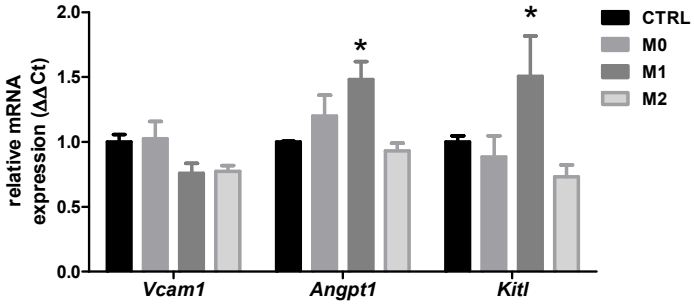

Supplemental figure 6. A) Expression of M1 (Il1b) and M2 (CD206) genes in M0, M1- and M2-polarized murine bone marrow macrophages for verification of in vitro polarization (*<0.05 versus M0). B) Gene expression of CD169 in mouse M0, M1- and M2-polarized macrophages (*p<0.05 versus M0). C) Ability of M0, M1 and M2 mouse macrophage conditioned medium to stimulate CXCL12 gene expression in mouse BM-derived MSCs (*p<0.05 versus M0). D) OSM protein concentrations, determined with ELISA, in conditioned media of M0, M1 and M2 murine macrophages (*p<0.05 versus M0).

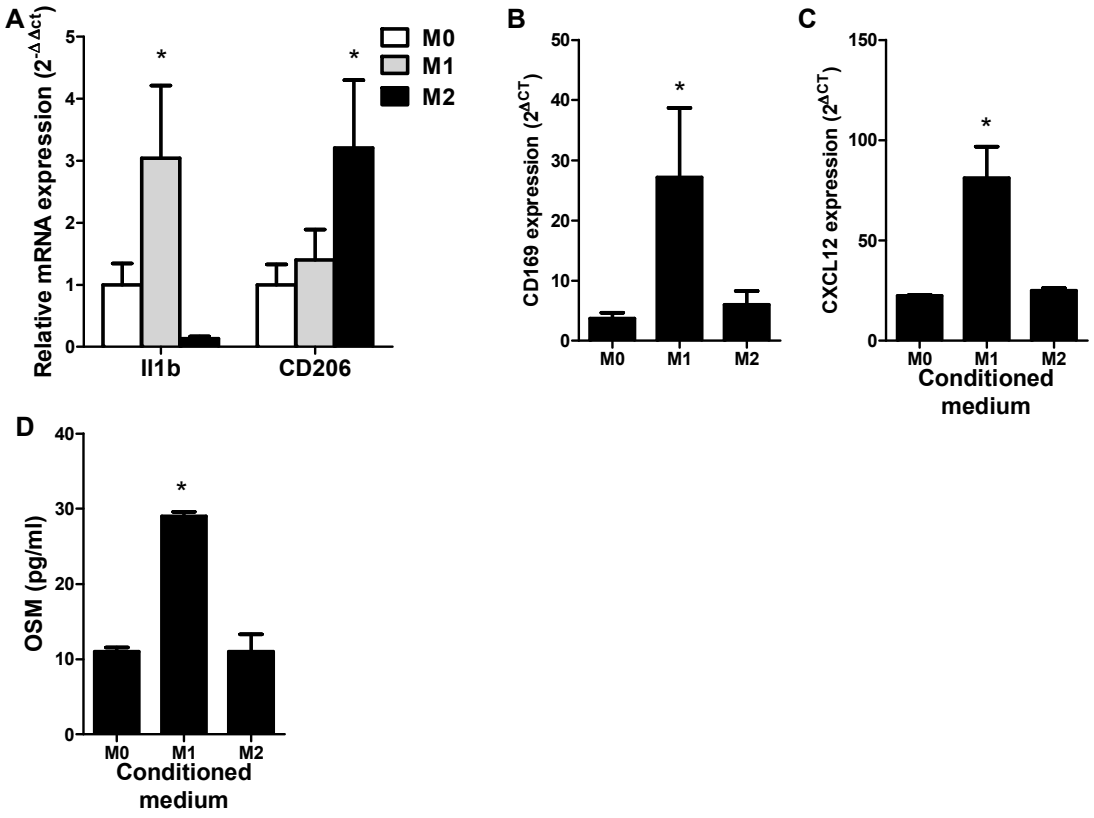

Supplemental figure 7. Strategy used for the in silico data mining approach to identify the macrophage (Mϕ) derived secreted protein that stimulates CXCL12 expression by MSCs. FC, fold change. B) A list of candidate factors retrieved by the method illustrated in A for further screening in vitro.

A

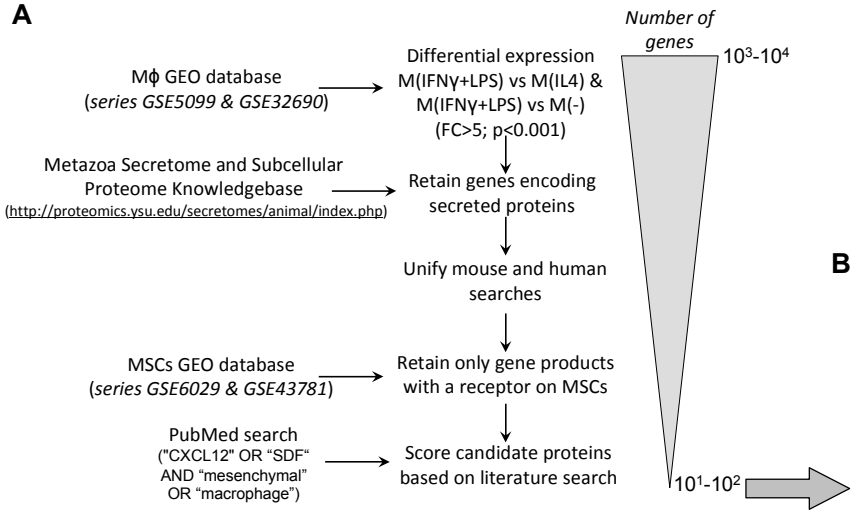

B

Gene	Product
BMP8B	Bone morphogenetic protein 8beta
C3	Complement C3
CCL19	Chemokine (C-C motif) ligand 19
CCL5	Chemokine (C-C motif) ligand 5
COCH	Coagulation factor C homolog
CSF3	Colony stimulation factor 3
CXCL10	Chemokine (C-X-C motif) ligand 10
CXCL11	Chemokine (C-X-C motif) ligand 11
CXCL9	Chemokine (C-X-C motif) ligand 9
EDN1	Endothelin-1
IFNB1	Interferon beta
IL12A	Interleukin-12alpha
IL12B	Interleukin-12beta
IL15	Interleukin-15
IL1F9	Interleukin 1 family, member 9
IL6	Interleukin-6
LTA	Lymphotoxin A
OSM	Oncostatin M
PDGFA	Platelet derived growth factor A
SCT	Secretin
SEMA3C	Semaphorin 3c
SST	Somatostain
TNF	Tumor necrosis factor

Supplemental figure 8. Effects of incubating MSCs with different concentrations of potential candidate factors on CXCL12 gene expression.

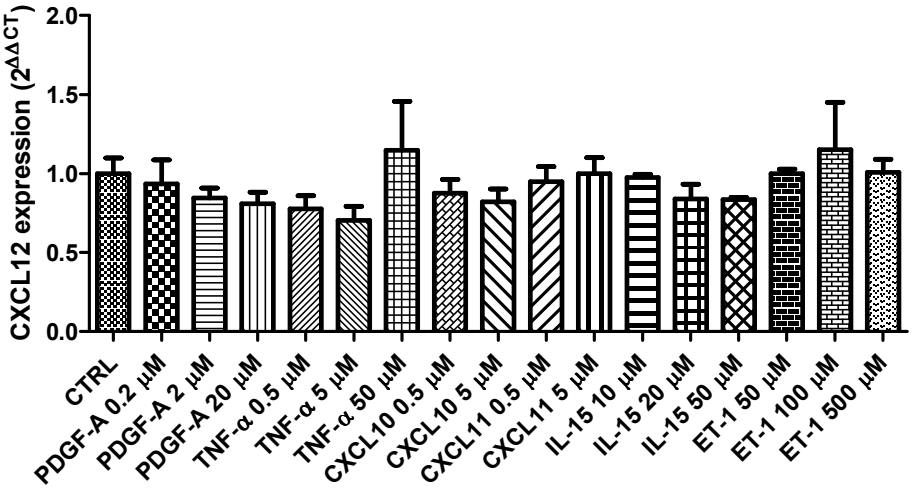

Supplemental figure 9. Effects of incubating MSCs with non-OSM gp130 ligands IL6 and LIF on CXCL12 gene expression.

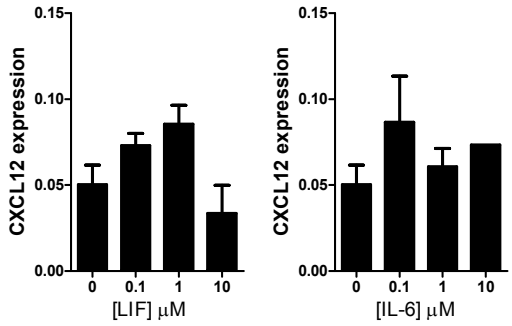

Supplemental Figure 10. A) Effects of OSM on CXCL12 induction in HUVECs, HAECs and fibroblasts. *p<0.05 versus CTRL. B) Effects of OSM on permeability of an endothelial monolayer. HUVES were grown at confluence and permeability of FITC-Dextran was assessed after 30 minutes and 2 hours as compared to fluorescence at baseline. Histamine was used as positive control. *p<0.05 versus CTRL at the same time point.

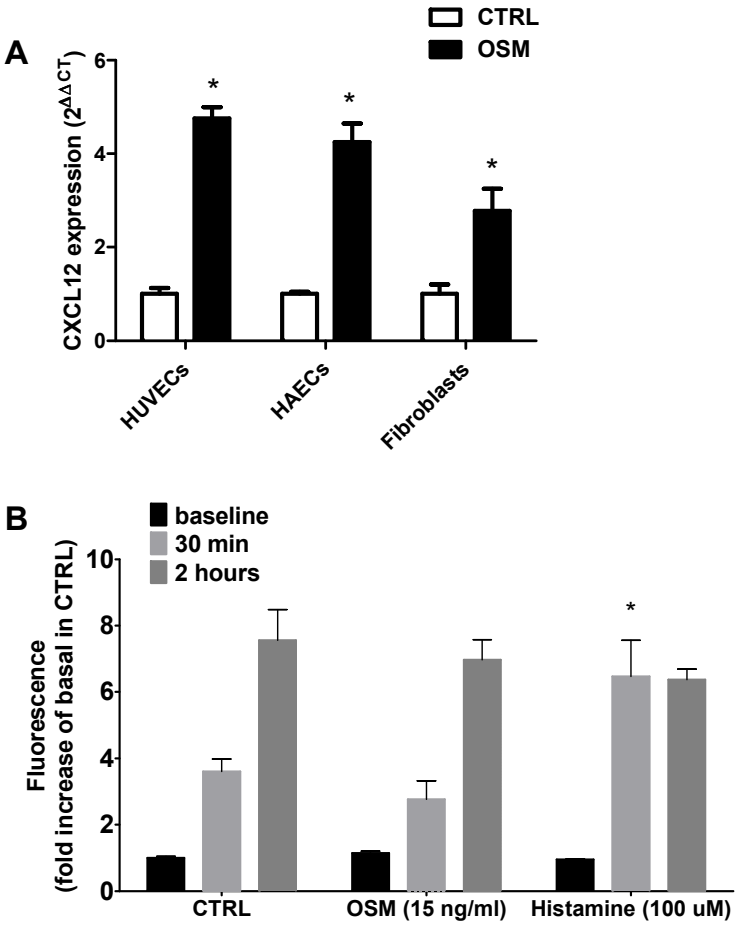

Supplemental Figure 11. OSM signalling pathway in MSCs. A) CXCL12 expression in MSCs incubated without or with OSM alone or in the presence of inhibitors of selected signalling pathways. *p<0.05 versus control (CTRL); #p<0.05 versus OSM. B) FACS analysis of STAT3 phosphorylation (meaning activation) in MSCs treated with OSM or with OSM + p38 inhibitor. C) CXCL12 expression in MSCs incubated without or with OSM and with p38 or STAT3 activators. *p<0.05 versus control (CTRL).

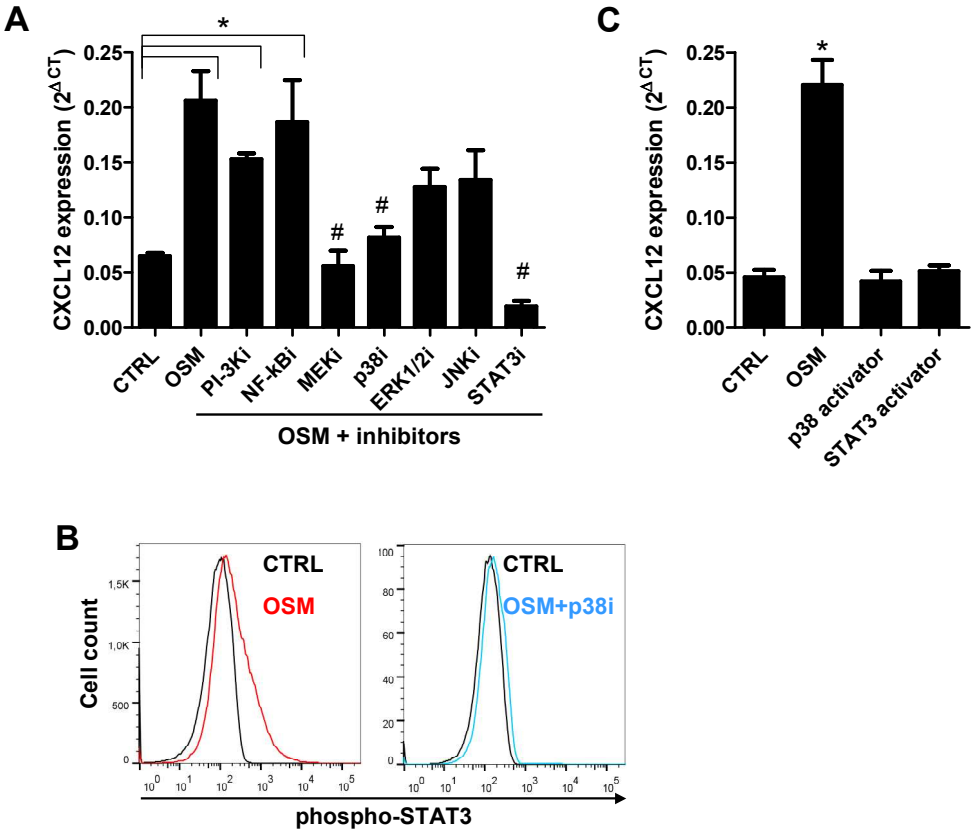

Supplemental Figure 12. Effects of OSM inhibition. A) Injection of an anti-OSM neutralizing antibody abated circulating OSM concentrations. *p<0.05 versus basal values. B) Injection of an anti-OSM neutralizing antibody before G-CSF stimulation restores the CXCL12 switch as shown by the PB/BM concentration ratio. When significantly (*p<0.05) different from 1.00, the PB-to-BM ratio of CXCL12 concentrations imply a mobilization gradient for SC toward the vasculature.

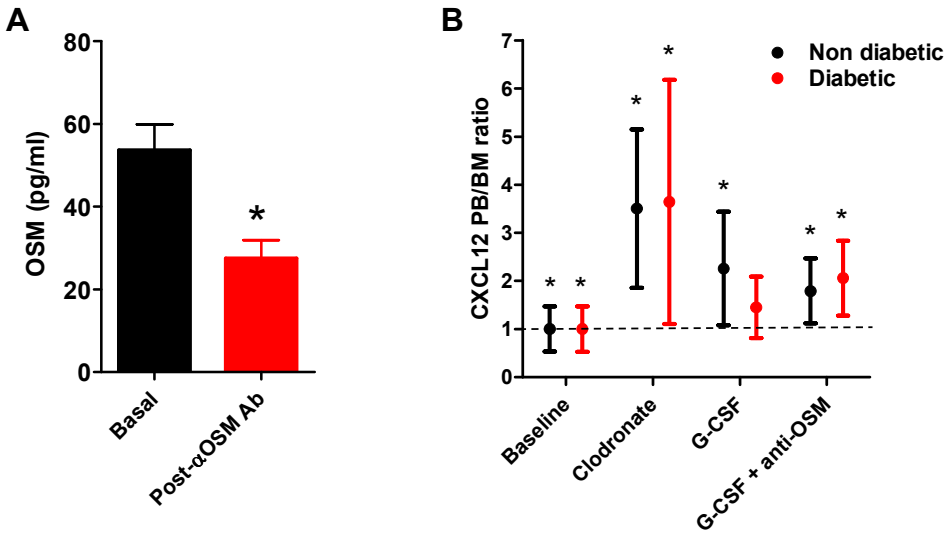

SUPPLEMENTARY DATA

Bone marrow macrophages contribute to diabetic stem cell mobilopathy by producing Oncostatin M

Additional details on patients recruitment and characterization. Subjects were enrolled provided they were free from any acute disease or infection and did not report active inflammatory conditions (e.g. rheumatic diseases), recent trauma or surgery, pregnancy/lactation. The following data were collected for all participants: age, sex, body mass index, history of hypertension, smoking habit, prevalence of cardiovascular disease, and medications. We also collected a fasting blood sample for determination of HbA1c and lipid profile, and a spot urinary sample for determination of albumin/creatinine ratio (ACR). Coronary artery disease (CAD) was defined as a past history of myocardial infarction or angina, or angiographic evidence of >50% obstruction of epicardial coronary arteries, or a positive myocardial perfusion stress test. Peripheral arterial disease (PAD) was defined in the presence of claudication or rest pain, or evidence of >50% obstruction in lower extremity arteries or an ankle-brachial index of less than 0.9. Cerebrovascular disease (CerVD) was defined as a past history of stroke or transient ischemic attack, or evidence of >30% carotid artery stenosis, or carotid endarterectomy. Prevalent atherosclerotic cardiovascular disease (CVD) was defined as either CAD, or PAD or CerVD isolated or in combination. In diabetic patients, we also recorded disease duration, prevalence of retinopathy (defined by digital funduscopic examination), neuropathy (defined by typical signs and symptoms, eventually confirmed by vibration perceptive threshold and/or electromyography), and nephropathy (defined as an albumin excretion rate >30 mg/g creatinine and/or estimated glomerular filtration rate <60 ml/min/1.73 m^2).

Additional details on animal protocols. Diabetes was induced with a single i.p. injection of 150 mg/kg STZ (Sigma Aldrich, St.Louis, MO, USA) in citrate buffer 50 mM, ph 4.5. Blood glucose was measured with Glucocard G-meter (Menarini, Florence, Italy); animals with blood glucose ≥300 mg/dl in at least two measurements within the first week were classified as diabetic and housed for 4 weeks with feeding and drinking ad libitum before performing experiments. Vav1-Sirt1$^{-/-}$ mice have been described previously (1). For SNS disruption, animals received intraperitoneal injections 100 mg/kg 6-hydroxy-dopamine (6-OHDA, Tocris Bioscience, Bristol, UK), as previously described (1).
Hind limb ischemia. Animals were sedated with 10 mg/kg zolazepam/thylamine (Zoletil®, Laboratories Virbac, Nice, France) and 7 mg/kg xylazine (Xilor®, Laboratories Carlier, Spain). The femoral artery and the vein were surgically dissected from the femoral nerve, then cauterized with low temperature cautery and excised between inguinal ligament and hackle. Stem/progenitor cell mobilization was assessed after 3 days, whereas we measured hind limb microvascular perfusion with Perimed Periscan-Pim II Laser Doppler System (Perimed AB, Sweden) and collected the limb muscles for analysis 14 days after surgery. In a separate batch of experiments (n≥3/group), animals were pretreated with the anti-OSM neutralizing antibody (αOSM) 24h before induction of ischemia.

Additional details on reagents. Antibodies. Monoclonal anti-mouse Ly-6G (Gr-1) PE (clone RB6-8C5, eBioscience, San Diego, CA, USA); monoclonal anti-mouse CD115 Alexa Fluor® 488 (clone AFS98, eBioscience); monoclonal anti-mouse F4/80 APC (clone BM8, eBioscience); monoclonal anti-human CD169 APC (clone 7-239, eBioscience); rat anti-mouse CD169 (clone MOMA-1, AbD Serotec, Oxford, UK). Citokines. Recombinant human Oncostatin M ; Recombinant human TNF-a; Recombinant human IL-6; Recombinant human RANTES; Recombinant human CXCL10; Recombinant human PDGF-AA; Recombinant human IL-4; Recombinant human IL-13; Recombinant human INF gamma; Recombinant human IL-15 all by PeproTech (Rocky Hill, NJ, USA). Recombinant human LIF Recombinant murine IL-4; Recombinant IL-13 and Recombinant INF-gamma were by Miltenyi Biotec (Cologne, Germany).

SUPPLEMENTARY DATA

Additional details on mobilization assays. G-CSF stimulation. Progenitor cell levels were quantified in peripheral blood after peripheral ischemia or after 4 days of s.c. injection of 200 μg/kg/die of hrG-CSF (Filgrastim, Roche, Basel, Switzerland). BM macrophage depletion. Clodronate liposomes were used to deplete BM macrophages and induce mobilization: 250 ul of clodronate liposome (ClodronateLiposomes.com, The Netherlands) were injected intravenously. Flow cytometry was performed on blood collected at basal and 24 hours after liposome administration. In separate experiments, clodronate liposomes were given 24 hours before beginning G-CSF administration as described above. Oncostatin M neutralization. The day before starting G-CSF stimulation, 100 μg of an anti-OSM antibody (AF-495-NA, R&D Systems) were injected intraperitoneally in diabetic and non diabetic mice.

Additional details on FACS analysis. Human samples. Circulating monocyte-macrophages were identified and quantified as previously described. Briefly, after red blood cell lysis, cells stained with FITC-conjugated anti-CD68 mAb (Dako) and PE-conjugated anti-CCR2 mAb (R&D Systems) for identification of M1 cells and with FITC-conjugated anti-CX3CR1 (Biolegend), PE-conjugated anti-CD163 (BD) and APC-conjugated anti-CD206 (BD) mAbs for M2. M1 were defined as $CD68^{+}CCR2^{+}$ cells and M2 were defined as $CX3CR1^{+}CD163^{+}/CD206^{+}$. Baseline and post-G-CSF levels of circulating $CD34^{+}$ stem cells were quantified as previously described (2).
Murine samples. For identification of murine BM macrophage phenotypes we used the protocol described by Chow et al. (3). Cells were isolated by flushing femurs and tibia. After red blood cell lysis, cells were stained with Gr-1 (Ly6C/G, eBiosciences), CD115 (eBiosciences), and F4/80 (eBiosciences). Macrophages were identified in the $Gr\text{-}1^{neg}/CD115^{neg}$ gate as cells expressing the macrophage marker F4/80 with low side scatter, to distinguish them from eosinophils. $Gr\text{-}1^{+}CD115^{-}$ neutrophils, $Gr\text{-}1^{high}CD115^{+}$ monocytes and $Gr\text{-}1^{-}CD115^{+}$ monocytes were also identified, scored and sorted, when needed for gene expression analyses, using a BD FACS-Aria instrument. In parallel experiments, macrophages were also identified as cells that co-expressed F4/80 and MHC-II (eBiosciences) in the $CD45^{+}Gr\text{-}1^{-}$ gate.
Progenitor cell levels were quantified in peripheral blood after peripheral ischemia (at day 3) or after 4 days of s.c. injection of 200 μg/kg/die of hrG-CSF (Filgrastim, Roche, Basel, Switzerland). 150 μl of peripheral blood were stained with rat anti-mouse APC-lineage cocktail (BD, NJ, USA), PE rat anti-mouse Sca-1 (Ly6A/E, BD) and FITC rat anti-mouse cKit (BD) to quantify LKS cells or with Alexa647 rat anti-mouse CD34 (BD) and Alexa488 anti-mouse Flk-1 (Biolegend, San Diego, CA, USA) to quantify endothelial-committed progenitors. A total of 250.000 events were acquired for each analysis and the level of progenitor cells was expressed as number of positive events per 1.000.000 total events. Data were acquired using a FACS Calibur instrument (BD Biosciences) and analyzed with FlowJo X (TreeStar Inc., USA). For identifying LKS cells in the ischemic muscles, the tissue was digested with collagenase and the cell suspension was analyzed by FACS: singlet, live (7-AAD negative) cells were gated for negative lineage markers and Sca-1 / c-kit expression as described above.

Additional data on cell culture. Human monocyte-derived macrophages. Venous blood was obtained from healthy donors and separated using a Ficoll-Paque solution (Sigma Aldrich). Mononuclear cells were collected, washed with PBS containing EDTA (5 mmol/L) and resuspended at 2×10^{6} cells/mL in RPMI-1640 supplemented with 2 mmol/L glutamine, 0.5% penicillin-streptomycin and 15% FCS. Monocytes were separated from lymphocytes by adherence to 100-mm plastic dishes for 2 hours at 37°C, 5% CO_2. Adherent monocytes were cultured in fresh medium for 7 days at 37°C to allow spontaneous differentiation into macrophages. At the end of the differentiation period, resting cells were polarized into M1 or M2 macrophages by 48h incubation with LPS (1 μg/ml) and IFN-γ (10 ng/ml) or IL-4 (20 ng/ml) and IL-13 (5 ng/ml), respectively.

SUPPLEMENTARY DATA

Generation of conditioned medium. After 48 hours polarization, the medium was removed. Macrophages were thoroughly washed with PBS and kept in serum-free RPMI for further 72 hours. Afterwards macrophage conditioned media (CM) were harvested, centrifuged at 4000 x g for 20 min, passed through a 0.22-μm filter to eliminate the cellular debris and then stored at -20 °C. For in vitro experiments, CM from M0, M1 and M2 macrophages were concentrated 10-fold using Centriplus filters with 3 kDa cut-off (Amicon) and used at 20% v/v.

Human bone marrow MSCs were obtain from the BM of patients undergoing orthopedic surgery at the University Hospital of Padova (Ethical Committee prot. n. 2868P). Aspirates were washed twice with ice-cold sterile PBS and the cell pellets were plated on TC Petri dishes (Beckton Dickinson) with complete mesenchymal medium (MesenCult plus Mesenchymal Stem Cell Stimulatory Supplements, Stem Cells technologies Inc.). The medium was changed when fibroblast-like cells began to appear and then every other day. Experiments were performed with MCS at passage 5 or lower.

Murine MSCs. MSC were obtained by from 3 months old male wild-type C56Bl6/J mice from in-house colony. Mice were euthanized and femurs and tibia removed. Under sterile condition, bones were carefully cleaned from tissue debris and flushed with ice cold PBS. Cells were plated on TC Petri dishes (BD) with MEM-alpha medium (Sigma Aldrich) supplemented with glutamine, penicillin-streptomycin and 15% FBS, until cells reached 70% confluence and then passed for expansion. For experiments, mMSC were used up to passage 6. Murine macrophages. Mouse BMM were obtained by flushing with sterile ice-cold PBS both femurs and tibia of 3 months old male wild-type C56Bl6/J mice. Red blood cells were lysed with Ammonium-Chloride-Potassium Lysing Buffer. To obtain resting macrophages, 150.000 cells/cm^2 were plated on tissue culture Petri dishes with RPMI-1640 medium supplemented with glutamine, penicillin-streptomycin and 10% FCS + 10 nM murine macrophage-colony stimulating factor (M-CSF, Miltenyi Biotech) for 7 days without any medium change. Thereafter, macrophages were polarized toward M1 or M2 phenotype by incubation for 48 h with lipopolysaccharide (LPS; 1 μg/ml) and IFN-γ (10 ng/ml) or IL-4 (20 ng/ml) and IL-13 (5 ng/ml), respectively. Medium was then changed with RPMI-1640 medium supplemented with glutamine, penicillin-streptomycin without serum for 48 hours to yield conditioned medium. For each batch of conditioned medium, at the end of the experiments BMM were collected and analyzed by flow cytometry or kept in Trizol® for gene expression analysis.

In addition to MSCs, in some experiments, HUVECs, HAECs and human fibroblasts were used to study the effects of OSM on CXCL12 expression. Previously described standard protocols were used to culture humans fibroblasts (4), HUVECs and HAECs (5).

Permeability assay. Permeability of an endothelial cell monolayer was evaluated using HUVECs grown at confluence on fibronectin according to the vascular permeability assay as described by Ma et al (6).

Technical details of gene expression analyses. Total RNA was extracted using Trizol® reagent and following the manufacturer's protocol. RNA quantity was determined by a Nanodrop Spectrometer (Thermo-Fisher Scientific Inc) (using 1 OD260 = 40μg RNA). A260/A280 ratios were also calculated for each sample. RNA was then reverse transcribed to generate cDNA using the First-Strand cDNA Synthesis Kit from Invitrogen® following the protocol provided by the manufacturer. Reverse Transcription was performed using 400 ng of RNA with the following reaction mix: 250 ng of random primers, 1 μl 10 mM dNTP Mix (10 mM each dATP, dGTP, dCTP and dTTP at neutral pH) and sterile, distilled water to 13 μl. The sample were mixed by vortexing, briefly centrifuged and denaturated by incubation for 5 minutes at 70°C to prevent secondary structures of RNA. Samples were incubated on ice for 2 minutes to allow the primers to align to the RNA and the following components were added sequentially: 4 μl 5X First-Strand Buffer, 1 μl 0.1 M DTT, 1 μl RNaseOUT™ Recombinant RNase Inhibitor, 1 μl of SuperScript™ III RT (200 units/μl), all by Invitrogen. At the end of reaction, the volume of each sample was adjusted to 40 μl with RNase free water. Duplicates of sample cDNA were

then amplified on the 7900HT Fast Real-Time PCR System (Applied Biosystems) using the Fast SYBR Green RT-PCR kit (Applied Biosystems) in 96-wells or 384-wells plates (Micro Amp Optical, Applied Biosystems) by adding: 4.8 µl of Fast SYBR Green master Mix, 0.2 µl Primer Mix (15 µM), 5.0 µl of diluted cDNA. Specificity of gene amplification was confirmed by analyzing the dissociation curve with SDS 2.3 software (Applied Biosystems). Expression data were normalized to the mean of housekeeping gene ubiquitin C to control the variability in expression levels and were analyzed using the 2(-ΔΔCT) method. Gene-specific primer pairs were designed using Primer-BLAST (NCBI) and were each validated prior to use by gradient PCR and gel analysis to test for optimal annealing temperature, reaction efficiency and specificity (Table S1).

Additional data on in vitro CXCL12 assays. Human and mouse MSC were plated on 6-well TC plates (BD) for each experiment. Upon reaching 90% confluence, cytokines and chemicals was added at given concentrations with Mesencult medium without supplements. Conditioned media were incubated with anti-Oncostatin M antibodies, mouse anti-human and rabbit anti-mouse (MAB295 and AF-495-NA respectively; R&D), at 37°C for 30 minutes and then added to the cells. Macrophage conditioned media were treated with 0.5 mg/ml proteinase K (Sigma-Aldrich, St. Louis, MO) for 30 min at 37°C and then heat inactivated at 95°C for 10 min and then added to MSC for 48 hours. All experiments were conducted for 48 hours and then cells were lysed with Trizol for gene expression analysis. For STAT3 phosphorylation experiments, we used Phosphoflow® PE Mouse Anti-Stat3 (pY705, BD) according to the manufacture's instruction.
CXCL12 protein was measured using the R&D Systems (DSA00 for human and MCX120 for mouse). OSM protein was quantified by ELISA (Raybiotech ELH-OSM for human; R&D MSM00 for mouse). To explore the pathways mediating effects of OSM on CXCL12 expression, we used the following chemicals. Inhibitors of p38 (SB202190), STAT3 (Stattic, S7024), JNK (SP600125), ERK 1/2 (SCH 772984) were from Selleckchem (Houston, TX, USA). Inhibitor of MEK (U0126) from Calbiochem, Millipore. Amlexanox (NF-kB inhibitor), colivelin and anisomycin were from Tocris (R&D Systems), protease inhibitor (P1860) and Pi3K inhibitor (Wortmannin) were from Sigma Aldrich.
Murine bone marrow sample were obtained by pulverizing 1 femur with liquid nitrogen and by adding 250 ul of ice-cold PBS with complete protease inhibitor cocktail (Roche, Basel, Switzerland). After orbital rotation at 4°C for 15 minutes, samples were centrifuged at 13300 RPM at 4°C and surnatants kept at -80°C for analysis.

Specific details of the in silico analyses. In silico analyses were performed retrieving data from GEO database. GSE32690 dataset was used to get murine expression data, and in particular we analyzed the following groups of samples: GSM812310, GSM812311, GSM812312 (M(-)); GSM812313, GSM812314, GSM812315 (M(IFNγ+LPS)); GSM812316, GSM812317; GSM812318 (M(IL-4)). GSE5099 dataset was used to get human expression data, grouped as follows: GSM115052, GSM115053, GSM115054, GSM115067; GSM115068, GSM115069 (M(-));GSM115055, GSM115056, GSM115057, GSM115070, GSM115071, GSM115072 (M(IFNγ+LPS)); GSM115058, GSM115059, GSM115060, GSM115073, GSM115074, GSM115075 (M(IL4)). Murine and human expression data were both divided in two different groups (M(-) or M0 vs M(IFNγ+LPS) or M1 and M(IL4) or M2 vs M(IFNγ+LPS) or M1, and then analyzed using GEO2R tool, selecting the Benjamini & Hochberg false discovery rate p-value adjustment. We subsequently filtered data according to these stringent criteria: being upregulated in M(IFNγ+LPS) verus M(-) and versus M(IL4) macrophages at least 5 folds (logFC>2.32), and with an adjusted p-value <0.001, in both groups. The two groups where then crossed, to get a list of genes commonly upregulated in M(IFNγ+LPS) macrophages. Since we were interested in secreted proteins, data were furthermore filtered by comparing the previous human and murine gene lists respectively with a specie-specific secreted protein list. These were obtained from

the Metazoa Secretome and Subcellular Proteome Knowledgebase (MetazSecKB, http://proteomics.ysu.edu/secretomes/animal/index.php), choosing the "Curated secreted" option for both human and murine list, after converting each of them from UniProt accession to official gene name with David conversion tool (http://david.abcc.ncifcrf.gov/conversion.jsp). We manually checked for proteins which have a known receptor. Finally, we compared this list with microarray expression data of human (GSM139891, GSM139892, GSM139893, GSM139907, GSM139908, GSM139909, part of GSE6029) and murine (GSM1071218, GSM1071219, GSM1071220, part of GSE43781) bone marrow derived mesenchymal stem cells, to check whether these receptors were expressed at any level.

References

1. Albiero M, Poncina N, Tjwa M, Ciciliot S, Menegazzo L, Ceolotto G, Vigili de Kreutzenberg S, Moura R, Giorgio M, Pelicci P, Avogaro A, Fadini GP: Diabetes causes bone marrow autonomic neuropathy and impairs stem cell mobilization via dysregulated p66Shc and Sirt1. *Diabetes* 63:1353-1365, 2014
2. Fadini GP, Albiero M, Vigili de Kreutzenberg S, Boscaro E, Cappellari R, Marescotti M, Poncina N, Agostini C, Avogaro A: Diabetes impairs stem cell and proangiogenic cell mobilization in humans. *Diabetes Care* 36:943-949, 2013
3. Chow A, Lucas D, Hidalgo A, Mendez-Ferrer S, Hashimoto D, Scheiermann C, Battista M, Leboeuf M, Prophete C, van Rooijen N, Tanaka M, Merad M, Frenette PS: Bone marrow CD169+ macrophages promote the retention of hematopoietic stem and progenitor cells in the mesenchymal stem cell niche. *J Exp Med* 208:261-271, 2011
4. Ceolotto G, Papparella I, Lenzini L, Sartori M, Mazzoni M, Iori E, Franco L, Gallo A, de Kreutzenberg SV, Tiengo A, Pessina AC, Avogaro A, Semplicini A: Insulin generates free radicals in human fibroblasts ex vivo by a protein kinase C-dependent mechanism, which is inhibited by pravastatin. *Free Radic Biol Med* 41:473-483, 2006
5. Albiero M, Rattazzi M, Menegazzo L, Boscaro E, Cappellari R, Pagnin E, Bertacco E, Poncina N, Dyar K, Ciciliot S, Iwabuchi K, Millioni R, Arrigoni G, Kraenkel N, Landmesser U, Agostini C, Avogaro A, Fadini GP: Myeloid calcifying cells promote atherosclerotic calcification via paracrine activity and allograft inflammatory factor-1 overexpression. *Basic Res Cardiol* 108:368, 2013
6. Ma C, Wang XF: In vitro assays for the extracellular matrix protein-regulated extravasation process. *CSH Protoc* 2008:pdb prot5034, 2008

SUPPLEMENTARY DATA

Supplementary Table 1. Primer sequences (m, mouse; h, human).

Gene	FW primer sequence	Rv primer sequence
m CD169	AAGTGTGCTGTATGCCCCAG	GGAACAGAGACAGGTGAGCC
m CD11c	TCTTCTGCTGTTGGGGTTTGT	GAGCACACTGTGTCCGAACT
m Cxcl12	GAGCCAACGTCAAGCATCTG	CGGGTCAATGCACACTTGTC
m nos2	TCCTGGACATTACGACCCCT	CTCTGAGGGCTGACACAAGG
m Tnfα	GTGGAACTGGCAGAAGAG	CCATAGAACTGATGAGAGG
m mrc1	TTGCACTTTGAGGGAAGCGA	CCTTGCCTGATGCCAGGTTA
m C5	CAGGGTACTTTGCCTGCTGA	TGGATTTTCATGGTGGGGCA
m Arg	ACAAGACAGGGCTCCTTTCAG	GGCTTATGGTTACCCTCCCG
m Mcp1	AGCTGTAGTTTTTGTCACCAAGC	GTGCTGAAGACCTTAGGGCA
h CD206	CCTCTGGTGAACGGAATGAT	AGGCCAGCACCCGTTAAAAT
h IL10	TACGGCGCTGTCATCGATTT	TGAGAGTCGCCACCCTGATGT
h IL1BETA	AACCTCTTCGAGGCACAAGG	GTCCTGGAAGGAGCACTTCAT
h CD169	TCGACGCTCAAGCTGTGAAT	CCATGTGTAGGTGAGCTGGG
h VCAM	GTTTGCAGCTTCTCAAGCTTTT	GATGTGGTCCCCTCATTCGT
h ANGPT	CAGACTGCAGAGCAGACCAGAA	CTCTAGCTTGTAGGTGGATAATGAATTC
h KITL	CGGGATGGATGTTTTGCCAAG	TTTCACGCACTCCACAAGGT
h CXCL12	ATGCCCATGCCGATTCTT	GCCGGGCTACAATCTGAAGG
h β-ACTIN	AGAGCTACGAGCTGCCTGAC	GGATGCCACAGGACTCCA

Supplementary Table 2. Characteristics of patients in the BM sub-study.

Variable	Non diabetic (n=6)	Diabetic (n=6)	p-value
Age, years	60.8±5.6	65.8±4.0	0.484
Sex male, %	83.3	100.0	0.340
Body mass index, kg/m1	24.5±1.5	29.0±2.0	0.161
Fasting plasma glucose, mg/dl	91.5±6.6	220.0±51.0	0.032
Hypertension, %	66.6	100.0	0.145
Systolic blood pressure, mm Hg	127.7±9.1	126.5±14.8	0.947
Diastolic blood pressure, mm Hg	64.7±4.1	75.7±6.8	0.197
Smoking habit, %	33.3	0.0	0.145
Total cholesterol, mg/dl	178.5±10.8	143.2±8.2	0.026
HDL cholesterol, mg/dl	51.3±5.0	40.8±4.1	0.134
LDL cholesterol mg/dl	109.3±13.9	72.2±7.5	0.040
Triglycerides, mg/dl	90.0±9.7	152.8±26.2	0.048
Medications			
Insulin, %	-	33.3	-
Oral antidiabetic agents, %	-	50.0	-
ACE inhibitors, %	100.0	83.3	0.340
Aspirin, %	83.3	83.3	1.000
Statin, %	50.0	66.6	0.599

SUPPLEMENTARY DATA

Supplementary Figure 1. A) Percentages of BM macrophages in control (CTRL) and sympathectomised mice treated with 6-OHDA. B) Percentages of BM macrophages in CTRL and hematopoietic (Vav-driven) Sirtuin-1 (Sirt1) knockout mice.

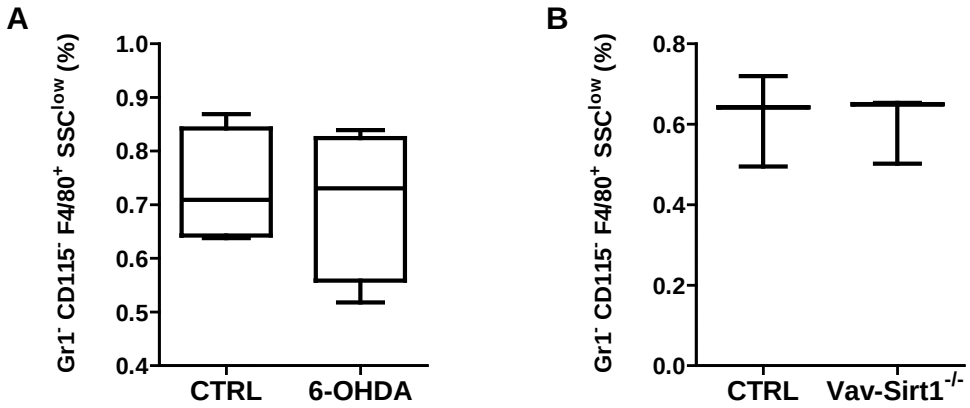

Supplementary Figure 2. Surface expression of CD169 was analyzed by FACS in BM cell populations identify by Gr-1, CD115 and F4/80 staining. Identity of the gated populations was confirmed by Hoechst nuclear staining morphology of sorted cells. The FACS histogram shows that CD169 is expressed at higher levels in macrophages compared to other populations.

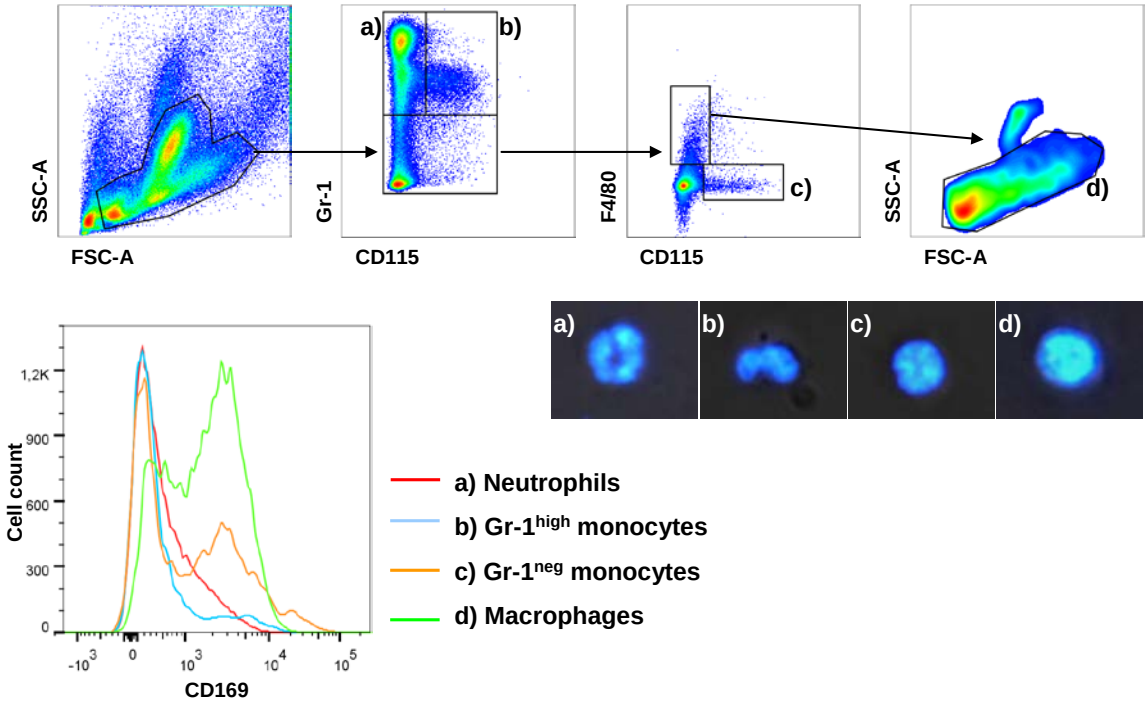

SUPPLEMENTARY DATA

Supplementary figure 3. A) Changes in PB Gr-1^{-}CD115^{-}F4/80^{+}SSC^{low} macrophages, BM Gr-1^{high} and Gr-1^{low} monocytes, as well as neutrophils after clodronate liposome treatment compared to baseline in non diabetic (CTRL) and type 1 diabetic (T1D) mice. B) Changes in niche gene expression in the whole BM after clodronate liposome treatment compared to baseline in CTRL and T1D mice. *p<0.05 versus baseline.

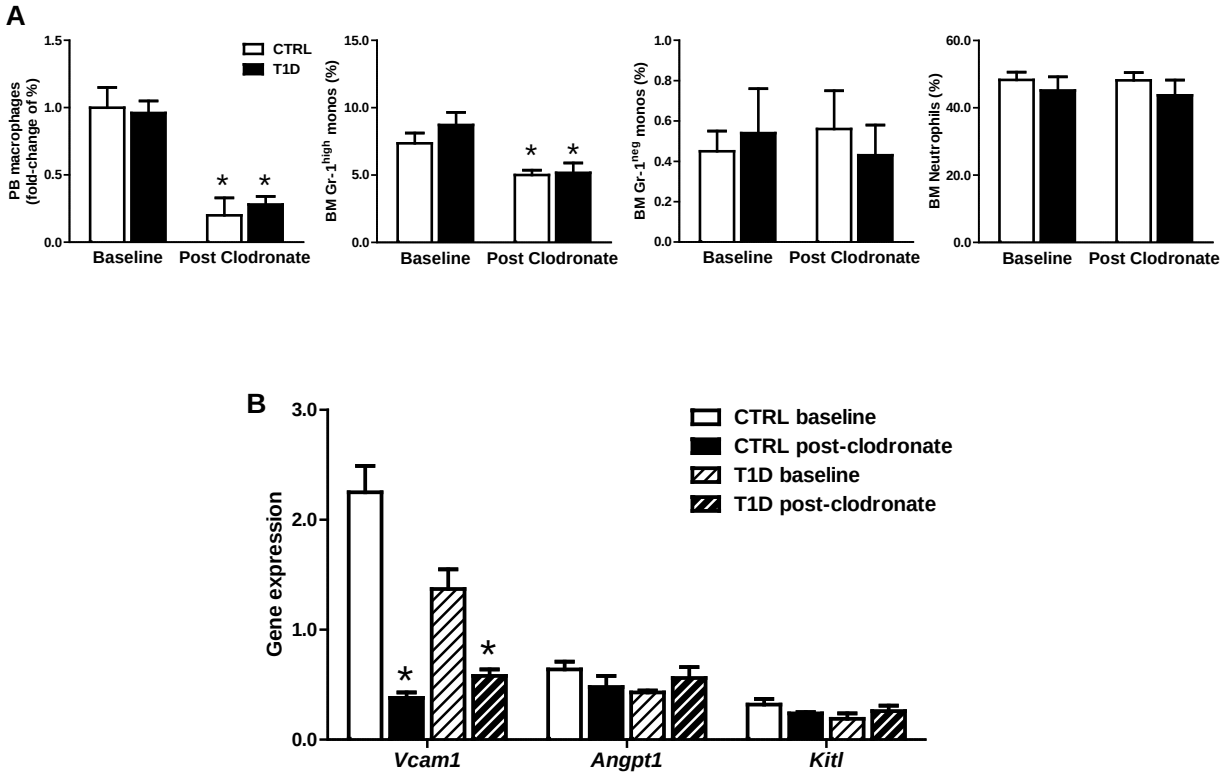

SUPPLEMENTARY DATA

Supplementary figure 4. Expression of typical M1 and M2 genes in cultured polarized macrophages, relative to expression in resting M0. *p<0.05 M1 versus M2.

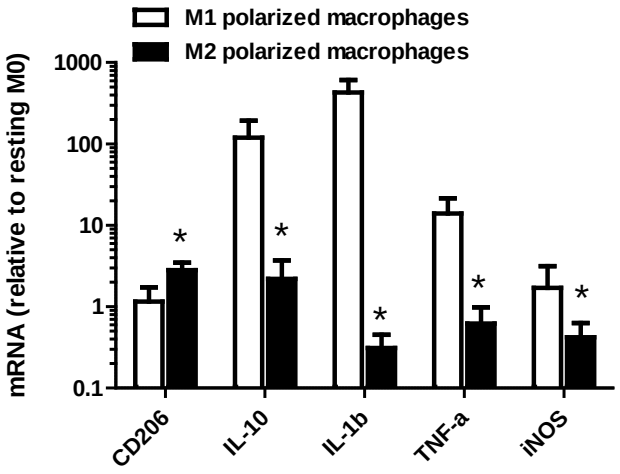

Supplementary Figure 5. Changes in the expression of niche genes in MSCs in the control condition (CTRL) or incubated with M0, M1 and M2 macrophage conditioned media. *p<0.05 versus CTRL.

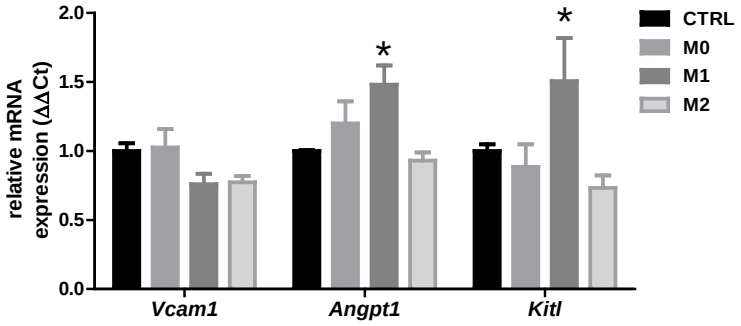

SUPPLEMENTARY DATA

Supplementary Figure 6. A) Expression of M1 (Il1b) and M2 (CD206) genes in M0, M1- and M2-polarized murine bone marrow macrophages for verification of in vitro polarization (*<0.05 versus M0). B) Gene expression of CD169 in mouse M0, M1- and M2-polarized macrophages (*p<0.05 versus M0). C) Ability of M0, M1 and M2 mouse macrophage conditioned medium to stimulate CXCL12 gene expression in mouse BM-derived MSCs (*p<0.05 versus M0). D) OSM protein concentrations, determined with ELISA, in conditioned media of M0, M1 and M2 murine macrophages (*p<0.05 versus M0).

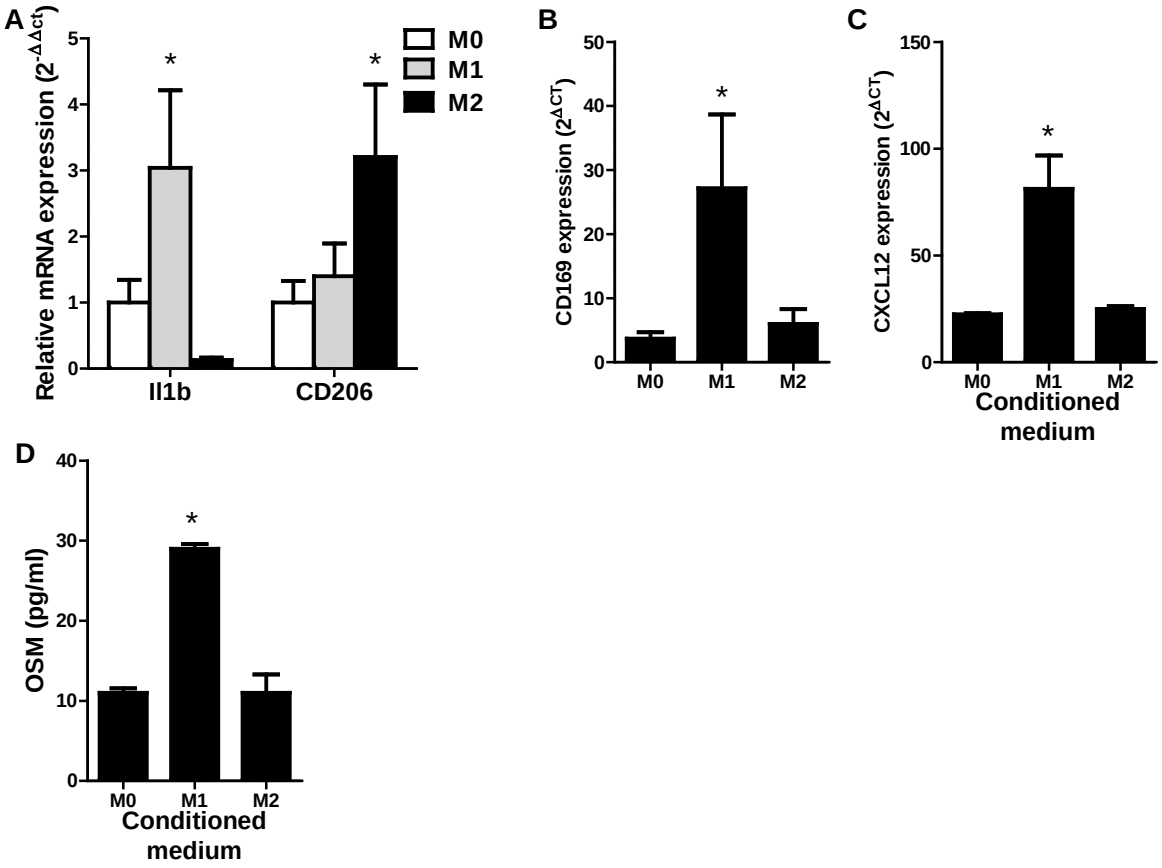

SUPPLEMENTARY DATA

Supplementary Figure 7. Strategy used for the in silico data mining approach to identify the macrophage (Mϕ) derived secreted protein that stimulates CXCL12 expression by MSCs. FC, fold change. B) A list of candidate factors retrieved by the method illustrated in A for further screening in vitro.

A

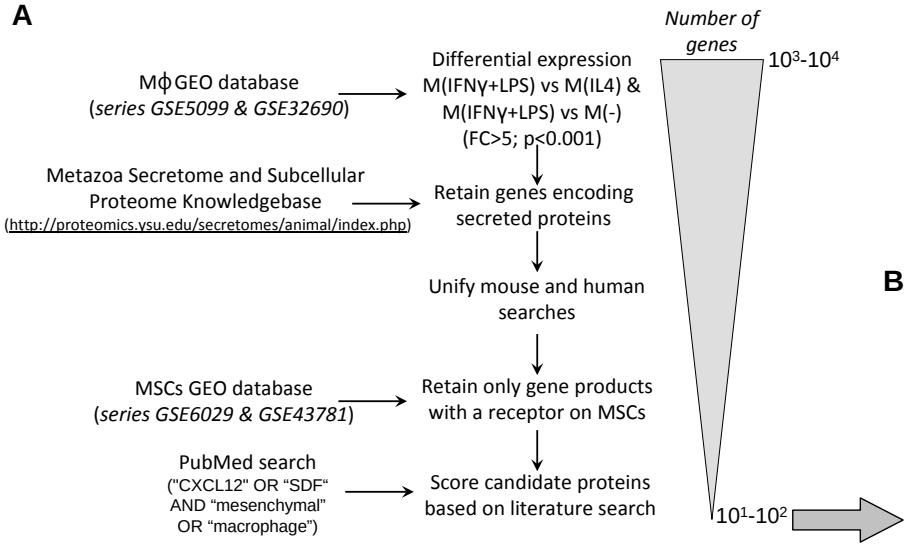

B

Gene	Product
BMP8B	Bone morphogenetic protein 8beta
C3	Complement C3
CCL19	Chemokine (C-C motif) ligand 19
CCL5	Chemokine (C-C motif) ligand 5
COCH	Coagulation factor C homolog
CSF3	Colony stimulation factor 3
CXCL10	Chemokine (C-X-C motif) ligand 10
CXCL11	Chemokine (C-X-C motif) ligand 11
CXCL9	Chemokine (C-X-C motif) ligand 9
EDN1	Endothelin-1
IFNB1	Interferon beta
IL12A	Interleukin-12alpha
IL12B	Interleukin-12beta
IL15	Interleukin-15
IL1F9	Interleukin 1 family, member 9
IL6	Interleukin-6
LTA	Lymphotoxin A
OSM	Oncostatin M
PDGFA	Platelet derived growth factor A
SCT	Secretin
SEMA3C	Semaphorin 3c
SST	Somatostain
TNF	Tumor necrosis factor

SUPPLEMENTARY DATA

Supplementary Figure 8. Effects of incubating MSCs with different concentrations of potential candidate factors on CXCL12 gene expression.

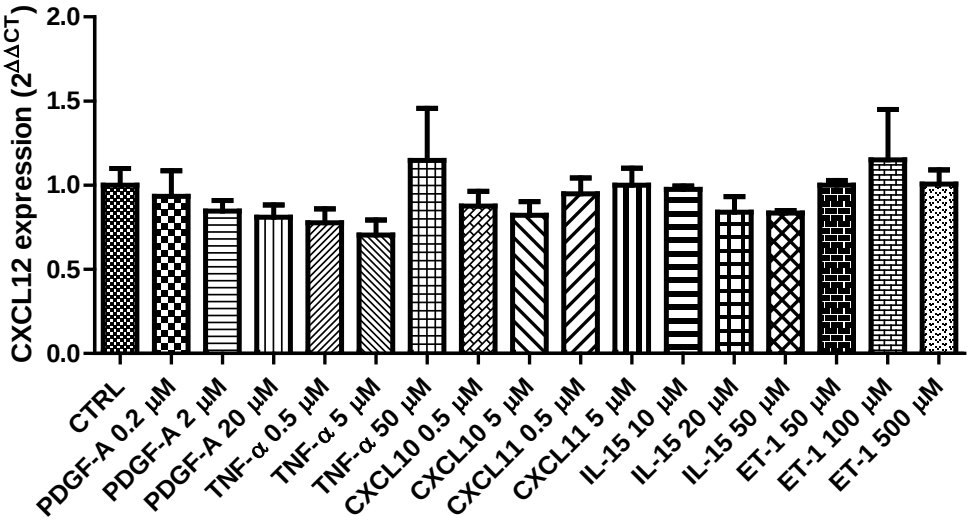

Supplementary Figure 9. Effects of incubating MSCs with non-OSM gp130 ligands IL6 and LIF on CXCL12 gene expression.

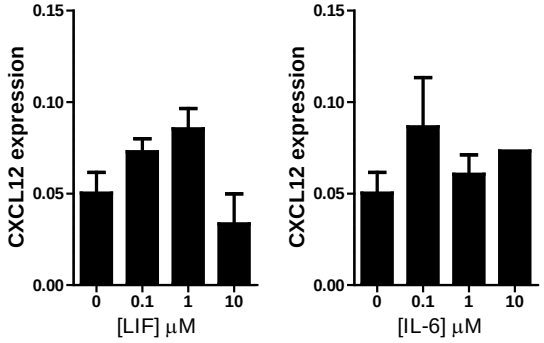

SUPPLEMENTARY DATA

Supplementary Figure 10. A) Effects of OSM on CXCL12 induction in HUVECs, HAECs and fibroblasts. *p<0.05 versus CTRL. B) Effects of OSM on permeability of an endothelial monolayer. HUVES were grown at confluence and permeability of FITC-Dextran was assessed after 30 minutes and 2 hours as compared to fluorescence at baseline. Histamine was used as positive control. *p<0.05 versus CTRL at the same time point.

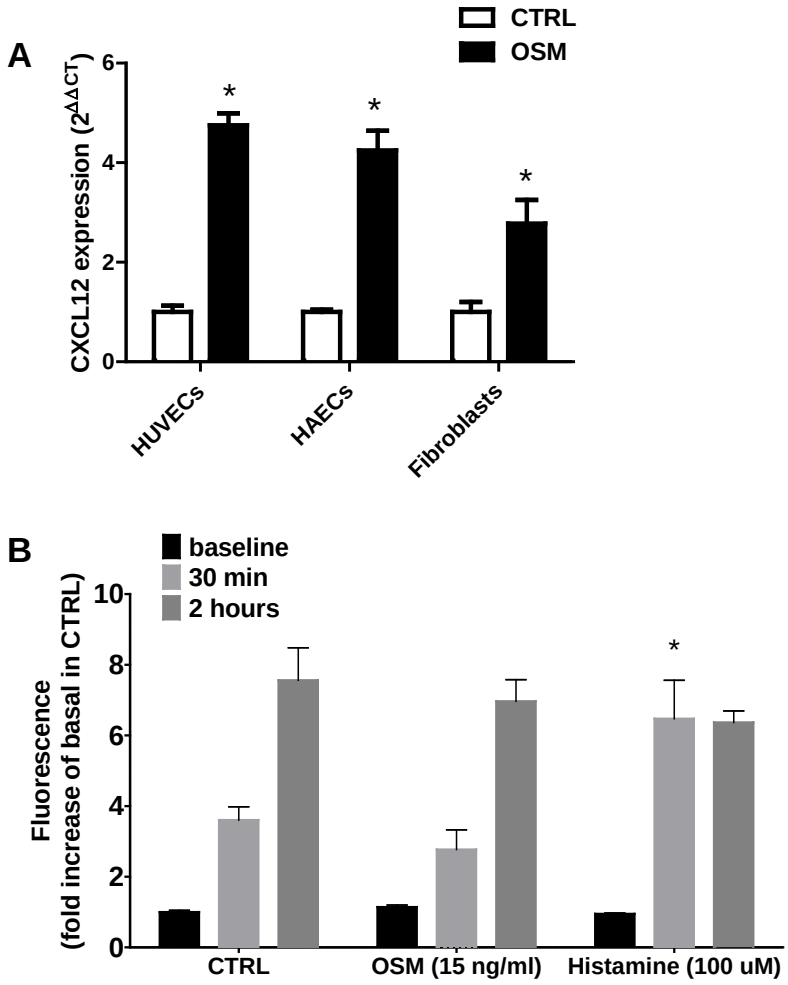

SUPPLEMENTARY DATA

Supplementary Figure 11. OSM signalling pathway in MSCs. A) CXCL12 expression in MSCs incubated without or with OSM alone or in the presence of inhibitors of selected signalling pathways. *p<0.05 versus control (CTRL); #p<0.05 versus OSM. B) FACS analysis of STAT3 phosphorylation (meaning activation) in MSCs treated with OSM or with OSM + p38 inhibitor. C) CXCL12 expression in MSCs incubated without or with OSM and with p38 or STAT3 activators. *p<0.05 versus control (CTRL).

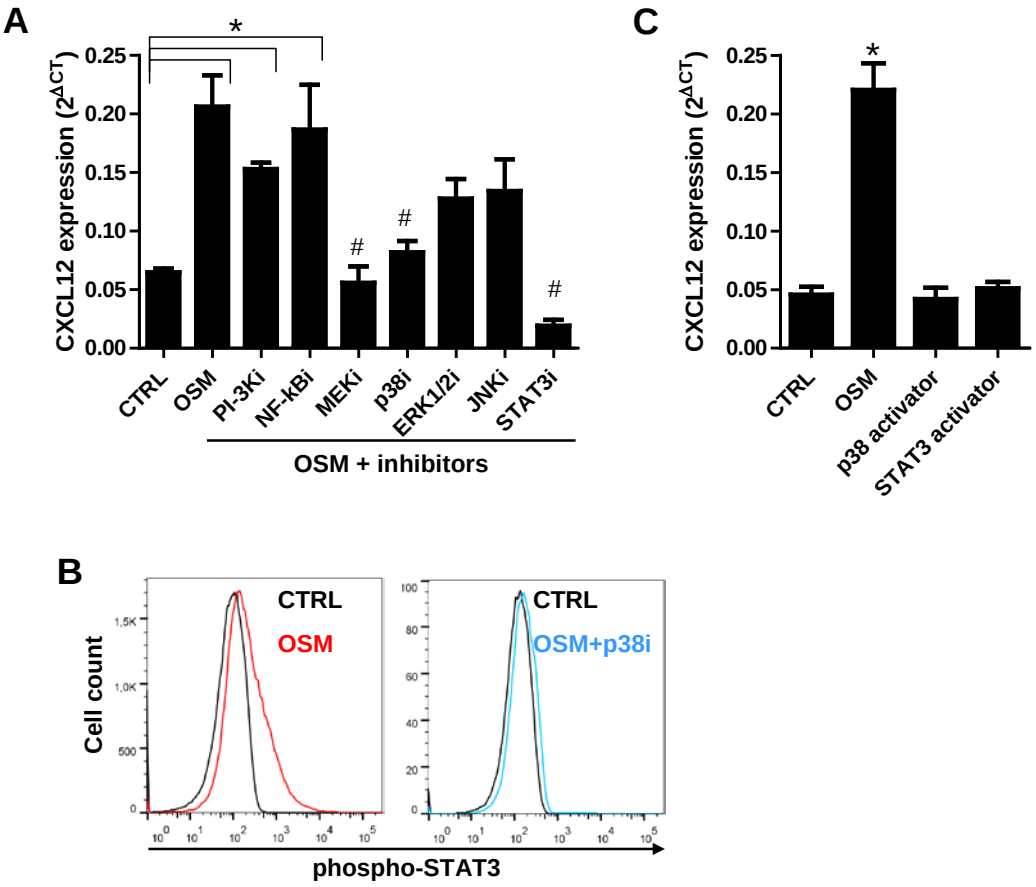

SUPPLEMENTARY DATA

Supplementary Figure 12. Effects of OSM inhibition. A) Injection of an anti-OSM neutralizing antibody abated circulating OSM concentrations. *p<0.05 versus basal values. B) Injection of an anti-OSM neutralizing antibody before G-CSF stimulation restores the CXCL12 switch as shown by the PB/BM concentration ratio. When significantly (*p<0.05) different from 1.00, the PB-to-BM ratio of CXCL12 concentrations imply a mobilization gradient for SC toward the vasculature.